



Faculty of Graduate Studies

Renewable Energy Management Master Program

**Bypass Diodes and Shade Tolerance of the
Road Integrated Photovoltaic Analysis**

Master Thesis

Submitted By

Sarah Rajab

Supervisors

Dr. Ahmed Abu Hanieh

Dr. Bart Pieters

15 Jan ,2024



Examination Committee Approval

Master Program in Renewable Energy Management

MSc. Thesis:

**Bypass Diodes and Shade Tolerance of the
Road Integrated Photovoltaic Analysis**

تحليل تأثير دايمود التجاوز على أداء خلايا الرصيف الشمسية في ظل
الظلال الجزئية

Student Name: Sarah Rajab (1205467)

This thesis was prepared under the main supervision of Dr. Ahmad Abu Haniah and has been accepted by all members of the examination committee.

Examination Committee:

Dr. Ahmad Abu Haniah	Signature
Dr. Mahran Qara'an (Member)	Signature
Dr. Ghassan Barghouthi (Member)	Signature

Date of Defense: 15 Jan, 2024

Dedication

الإهداء

أهدي هذه الرسالة للإطال وشهداء غزة، الذين أهدوا بجسارتهم وتحديهم أمام
الصعاب الكبيرة. لي أولئك الذين ضحوا بأرواحهم من أجل العدالة والحرية، والذين
استمروا في النضال من أجل غزة ولنضال الشعب الفلسطيني بشكل عام. هؤلاء
الإطال والشهداء هم مصدر إلهام لنا جميعاً، وستظل ذكراهم حية دائماً في قلوبنا
وفداً كرتنا.

أتمنى من الله أن يجعل رحمته وبركته تغشى على أرواحهم وأن يمن على عائلاتهم بالصبر
والقوة. هذه الرسالة هي تقدير واعتراف بتضحياتهم وتضامناً مع أهل غزة في رحلتهم
نحو العدالة والسلام. ندعو من أجل السلام والاستقرار في غزة وفلسطين، ونتطلع إلى يوم
يسود فيه السلام والأزدهار في هذه الأرض المقدسة.

To my family and friends who first believed I

can . . .

“I’ve learned that fear limits you and your vision. It serves as blinders to what may be just a few steps down the road for you. The journey is valuable, but believing in your talents, your abilities, and your self-worth can empower you to walk down an even brighter path. Transforming fear into freedom - how great is that?”

Soledad O’Brien

ACKNOWLEDGMENT

The present Master thesis is part of the framework of Palestinian German Science Bridge (PGSB), which is a pilot project financed by the German Federal Ministry of Education and Research (BMBF) and implemented jointly by Forschungszentrum Jülich GmbH (FZJ) and Palestinian Academy for Science and Technology (PALAST). I would like to thank Prof. Ahmed Abu Hanieh and Prof. Uwe Rau for giving me the opportunity to do my MSc thesis at IEK-5. Dr. Bart Pieters for his patient guidance, encouragement and advice throughout my time in Jülich. All the technicians I have been extremely lucky to work with all of you, I would like to express the deepest for all of you for your support and valuable feedback during the thesis study.

ABSTRACT

The principal objective of this study is to explore the ramifications of partial shading and the soiling model on the power generation of RIPV system. Specifically, the investigation delves into the impact of these factors in the presence or absence of Multilevel Bypass Diodes (MLBD) ,electrical Ng spice simulation model has been developed using irradiance model data these data was collected using Digital Elevation Model (DEM) called LiDAR and weather stations , which were simulated using SSDP software to analyze and make comparative analysis the impact of different shading condition and study the effect of MLB diodes on the partial shading RIPV modules, and the effect of MLB diodes in the soiling model. The results of this study illuminate the capacity of Multi-level Bypass diodes to overcome the challenges presented by soiling and partial shading effects within RIPV projects, where it appears that there is no significant impact in the case of partial shading, and there is a minimal effect on the panels in the case of dust affecting small particles. The significant impact was evident in the scenario of large particles (R= 5cm), where it greatly improves their productivity by up to 122.9% relative to the shading case. This understanding is pivotal in assessing the viability of incorporating bypass diode functionality to enhance the power efficiency and energy productivity

المستخلص

في هذه الأطروحة تم دراسة وتحليل تأثير الظلال الجزئية على أنظمة الطاقة الشمسية المتكاملة على الطرق بالتحديد، ودراسة تأثير الغبار والتربة عليها. تم جمع بيانات واحداثيات بالموقع من خلال مصدر لاحداثيات المواقع والتضاريس LidAR (DEM) حيث انه متوفر بشكل مجاني في ألمانيا في منطقة تواجد الألواح وكذلك معلومات الاشعاع الشمسي من خلال محطات الطقس لبناء نموذج للاشعاع الشمسي عبر برنامج SSDP، بعد ذلك استخدام نموذج الاشعاع الشمسي وعمل نمذجة كهربائية لهذه الألواح عبر برنامج ng-spice لمعرفة كمية الطاقة الناتجة في الحالات المختلفة للألواح الشمسية، ثم اضافة دايود التجاوز للبرنامج بعدة تصاميم لمعرفة كيفية تأثيره على انتاجية الألواح واجراء تحليل ومقارنة في الحالات السابقة.

نتائج هذه الدراسة تسلط الضوء على قدرة دوائر التجاوز متعددة المستويات على التغلب على التحديات التي تطرأ نتيجة لتأثيرات التلوث والظلال الجزئية في مشاريع الألواح الشمسية المتكاملة على الطرق، حيث يظهر أنه لا يوجد لها تأثير كبير في حالة الظلال الجزئية، ويكون التأثير ضئيل على الوحدات الشمسية في حالة وجود الغبار الناتج عن الجسيمات الصغيرة. كما ظهر التأثير بشكل كبير في سيناريو الجسيمات الكبيرة بقطر (5 سم)، حيث يعزز إنتاجيتها بشكل كبير يصل إلى 122.9٪ بالنسبة للحالة المظلمة. هذه النتائج مهمة في تقييم الجدوى الاقتصادية لإضافة دايود التجاوز لتعزيز كفاءة الطاقة والقدرة الإنتاجية.

Abbreviations

SSDP	the Simple Sky Dome Projector Software Program
DHI	diffuse horizontal irradiance
GHI	global horizontal irradiance
RIPV	Road Integrated PV
BIPV	Building Integrated PV
AWSM	All Weather Sky Model
POA	Plane of Array
SPA	the Solar Position Algorithm
SPICE	Simulation Program with Integrated Circuit Emphasis
STC	Standard Test Condition
MLBD	multi-level bypass diodes
PV	Photovoltaics
BPD	Bypass Diode
DC	Direct Current
AC	Alternative Current
VIPV	Vehicle Integrated PV
GW	Giga Watt
PMMA	polymethyl methacrylate
PR	Performance Ratio
I-V	Current -Voltage curve
DEM	Digital Elevation Model
LiDAR	high-resolution light detection and ranging
T	Temperature
Nb	Number of bypass diodes
CFF	Coverage Fraction Factor
O&M	Operations and Maintenance

Table of Contents

Contents

ACKNOWLEDGMENT	5
ABSTRACT	6
المستخلص	7
Abbreviations.....	8
Table of Contents	9
List of Figures.....	11
List of Tables	12
1 : Introduction	13
1.1 Background and Motivation	13
1.1.1 Renewable Energy and PV projects.....	13
1.1.2 Road Integrated Photovoltaic.....	16
1.1.3 Partial Shading, Soiling Factor and Bypass Diodes.....	18
1.2 Problem Statement.....	21
1.3 Thesis Questions	22
1.4 Thesis Organization.....	22
2 :Literature Review	24
2.1 RIPV	24
2.2 Partial shading, Soiling Effect and Bypass Diodes	28
3 : Approach and methodology	35
3.1 RIPV Performance Simulation	36
3.2 SPICE Simulation and Modeling of Bypass Diodes to Mitigate Partial Shading Effect	44
3.2.1 Concept and algorithm of Modelling MLB diodes:.....	47
3.3 Soiling Model	48
4 : Results	51
4.1 Partial Shading effect data analysis	51

4.2	Modeling and Simulation of adding MLBD Configuration:	53
4.3	Soiling Model and Simulation Result	57
4.4	Discussion of results	63
5	: Cost Analysis.....	65
5.1	Introduction:.....	65
5.2	4.2 Cost Components:.....	65
5.3	4.3 Operational and Maintenance Costs:	65
5.4	4.4 Key Financial Metrics Analysis	66
6	: Conclusion and Recommendation.....	69
6.1	5.1 Conclusion	69
6.2	5.2 Recommendations.....	70
	References.....	72

List of Figures

FIGURE 1.1 GLOBAL SOLAR PV CAPACITY FOR THE TOP 10 COUNTRIES AND THE REST OF THE WORLD IN 2021[2].	15
FIGURE 1.2 SOLAR PV GLOBAL CAPACITY SHARES OF TOP COUNTRIES AND REST OF WORLD, 2021 [2]	15
FIGURE 1.3 THE BASIC CONSTRUCTION OF THE RIPV MODULES. (REF)	17
FIGURE 3.1 THE SERIES CONNECTION BETWEEN SOLMOVE (8) MODULES	37
FIGURE 3.2 THE (36) SERIES CONNECTED CELL FOR EACH MODULE	38
FIGURE 3.3 SILICON WAFER RIPV WITH CAPACITY (0.304 kWp) ,SOLMOVE (38 wp),8 MODULES INSTALLED	38
FIGURE 3.4 THE STRUCTURE OF THE RIPV MODULES PROJECT IN JULICH.....	39
FIGURE 3.5 TOPOGRAPHY FOR THE RIPV AND THE STAFF AROUND, IN THE JULICH RESEARCH CENTER CAMPUS	40
FIGURE 3.6 THE IMAGE OF IRRADIANCE AND SHADING FOR THE STAFF AROUND WITH HIGH RESOLUTION, THE RED SQUARE PRESENTS THE RIPV MODULES	41
FIGURE 3.7 PV IRRADIANCE MODELING USING SSDP SOFTWARE TAKING INTO ACCOUNT THE DEM.....	42
FIGURE 3.8 SPICE MODEL SIMULATION INPUTS AND OUTPUTS IMPLEMENTATION	43
FIGURE 3.9 SCHEMATIC DIAGRAM OF THE COLLECTED DATA USED IN THE SPICE SIMULATION.	47
FIGURE 3.10 THE ASSUMPTION MODEL OF SMALL PARTICLES OF (1CM) RADIUS DISTRIBUTED OVER THE MODULES ..	49
FIGURE 3.11 THE ASSUMPTION MODEL OF BIG PARTICLES (R=5CM) ,CFF = 10% DISTRIBUTED OVER THE RIPV MODULES	50
FIGURE 4.1 PARTIAL SHADING EFFECT IN POWER GENERATION FOR THE ROAD INTEGRATED PHOTOVOLTAIC (RIPV) SYSTEM DURING JANUARY 2015 FOR 8 MODULES	51
FIGURE 4.2 OPTIMAL OUTPUT POWER OF THE ROAD INTEGRATED PHOTOVOLTAIC (RIPV) SYSTEM, REPRESENTING THE PEAK PRODUCTIVITY IN JUNE 2015 USING 8 MODULES.	52
FIGURE 4.3 PARTIAL SHADING IMPACT ON THE ROAD INTEGRATED PHOTOVOLTAIC (RIPV) SYSTEM IN DECEMBER 2015	53
FIGURE 4.4 MLB DIODES WITH VARIED CONFIGURATION DESIGNS A, B, C, D CONSEQUENTLY.	54
FIGURE 4.5 THE IMPACT OF PARTIAL SHADING IN FEBRUARY ACROSS VARIOUS WEATHER MODELS AND THE INFLUENCE OF INCORPORATING DIFFERENT CONFIGURATION DESIGNS MLB DIODES	55
FIGURE 4.6 ANNUAL ENERGY YIELDS PRODUCED BY ALL MODULES ACROSS VARIOUS WEATHER MODELS, AND WITH DIVERSE (MLB) DIODE CONFIGURATIONS IN STANDARD CONDITIONS (WITHOUT SOILING MODEL).....	55
FIGURE 4.7 THE ANNUAL POWER GENERATION FOR ALL MODULES ACROSS VARIOUS WEATHER MODELS UNDER STANDARD CONDITIONS (EXCLUDING SOILING MODEL).....	56
FIGURE 4.8 THE ANNUAL POWER GENERATION FOR ALL MODULES ACROSS VARIOUS WEATHER MODELS AND WITH DIVERSE (MLB) DIODE CONFIGURATIONS, CONSIDERING THE SOILING MODEL ASSUMPTION (R=1 CM)	58
FIGURE 4.9 ENERGY YIELD FROM ALL MODULES ACROSS VARIOUS WEATHER MODELS, AND WITH DIVERSE (MLB) DIODE CONFIGURATIONS, INCORPORATING THE SOILING MODEL (1 CM)	59
FIGURE 4.10 THE ANNUAL POWER GENERATION FOR ALL MODULES ACROSS VARIOUS WEATHER MODELS, CONSIDERING THE SOILING MODEL (5 CM) AND (MLB) DIODE CONFIGURATIONS.....	60
FIGURE 4.11 ENERGY YIELDS GENERATED BY ALL MODULES ACROSS VARIOUS WEATHER MODELS, INCORPORATING DIFFERENT (MLB) DIODE CONFIGURATIONS, CONSIDERING THE SOILING MODEL (5 CM)	60
FIGURE 4.12 THE ACQUIRED ENERGY YIELD IN THE PRESENCE OF SOILING CONDITIONS (5 CM) WAS ASSESSED BY INTRODUCING DISTINCT DESIGNS OF MLB DIODES DENOTED AS A, B, C, AND D.	63
FIGURE 4.13 YIELDS ENERGY GENERATED FROM ALL THE MODULES FOR THE DIFFERENT WEATHER MODELS USING MLB DIODES CONFIGURATION DESIGNS	64

List of Tables

TABLE 1-1-1 POLLUTANT EMISSION FACTORS FOR ELECTRIC GENERATION [1]	ERROR! BOOKMARK NOT DEFINED.
TABLE 3-1 THE DATASHEET FOR THE SOLMOVE MODULES, CRYSTALLINE WAFER SILICON MODULES.	45
TABLE 3-2 CHARACTERISTIC PARAMETERS USED IN THE SPICE SIMULATION MODEL FOR THE SOLAR CELL.....	46
TABLE 4-1 THE YIELD ENERGY YIELD FOR ALL THE WEATHER MODELS AND DIFFERENT CONFIGURATION OF MLB DIODES FOR THE 8 MODULES (STANDARD CASE) WITHOUT SOILING FACTOR.	56
TABLE 4-2 THE YIELD ENERGY FOR THE DIFFERENT WEATHER MODELS WHEN ADDING THE DIFFERENT DESIGN CONFIGURATION OF MLB DIODES WITH SOILING DISTRIBUTION OF 10 % COVERAGE FRACTION FACTOR, AND SOILING R=1 CM ,5 CM SUCCESSIVELY.....	62
TABLE 4-3 THE ENERGY YIELD GAIN AS A RESULT OF ADDING MLB DIODES CONFIGURATION DESIGNS.....	62
TABLE 5-1 KEY PARAMETERS AND FINANCIAL METRICS FOR THREE DISTINCT SCENARIOS OF A SOLAR PROJECT	67

1 : Introduction

1.1 Background and Motivation

1.1.1 Renewable Energy and PV projects

The development of clean energy resources to replace fossil fuels has become a crucial objective of modern science, engineering, and technology in the 21st century. The Kyoto Protocol highlighted the need to curb and reduce air pollution caused by the excessive and uncontrolled consumption of fossil fuels, and to maintain the ecological cycles of the biosystems on Earth. Among the various renewable energy resources and projects underway, photovoltaic (PV) solar energy has emerged as the most promising future energy technology due to its low CO₂ emission compared to other energy sources, as shown in Table 1.1. In contrast to coal, which produces 322 grams of CO₂ per 1 kWp, 1 kWp of PV generates only about 5 grams of CO₂. Additionally, the affordability of PV modules makes it an environmentally friendly and economically sustainable solution for investment in projects more than any other resources [1].

Table 1-1 Pollutant emission factors for electric generation [1]

Energy Source	CO₂ (g/kWh)
Coal	322.5
Oil	258.5
Natural Gas	178
Nuclear	7.5
Photovoltaic	5.3
Solar Thermal	3.3
Hydropower	5.9

Photovoltaic (PV) energy is a type of renewable energy that can be converted into electricity through the use of solar photovoltaic (PV) modules. PV modules utilize sunlight to generate current and voltage (DC), which can then be converted to (AC) using inverters for synchronization with the grid. In locations where a grid is unavailable, PV modules can be paired with batteries for energy storage, which makes them a cost-effective solution. The widespread design and installation of PV projects on a large scale can help reduce dependence on other polluting and unsustainable energy sources. The growing solar industry also creates a demand for skilled workers, engineers, and researchers.

The capacity of photovoltaic (PV) solar energy generation has increased by an average of 41% per year since 2009, with a total of 295 GW installed worldwide as of the end of 2022. This growth was accelerated during the Russian-Ukrainian conflict, as many countries were reliant on Russian gas. Asia has dominated all other regions in terms of new solar PV installations for the ninth consecutive year, representing 52% of the global added capacity in 2021. The Americas (21%) surpassed Europe (17%) in new installations. The top five countries for newly installed capacity were China, the United States, India, Japan, and Brazil, which together accounted for approximately 61% of the total newly installed capacity (Figures 1.1 and 1.2). However, this top share was lower than in 2020 due to increasing competition in response to declining capital and operational costs of solar PV[2].

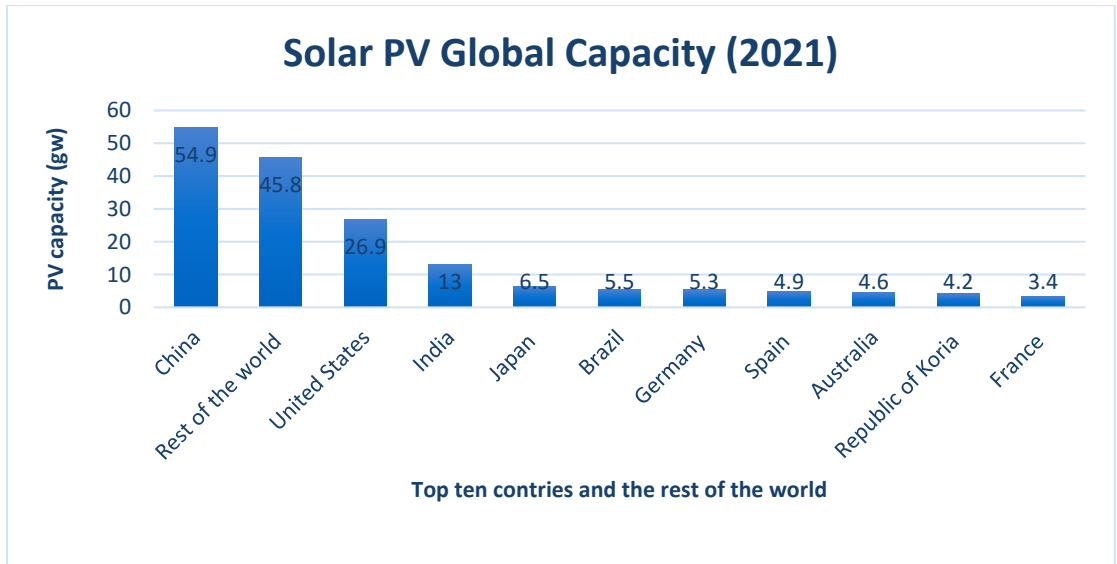


Figure 1.1 Global Solar PV Capacity for the Top 10 Countries and the Rest of the World in 2021[2].

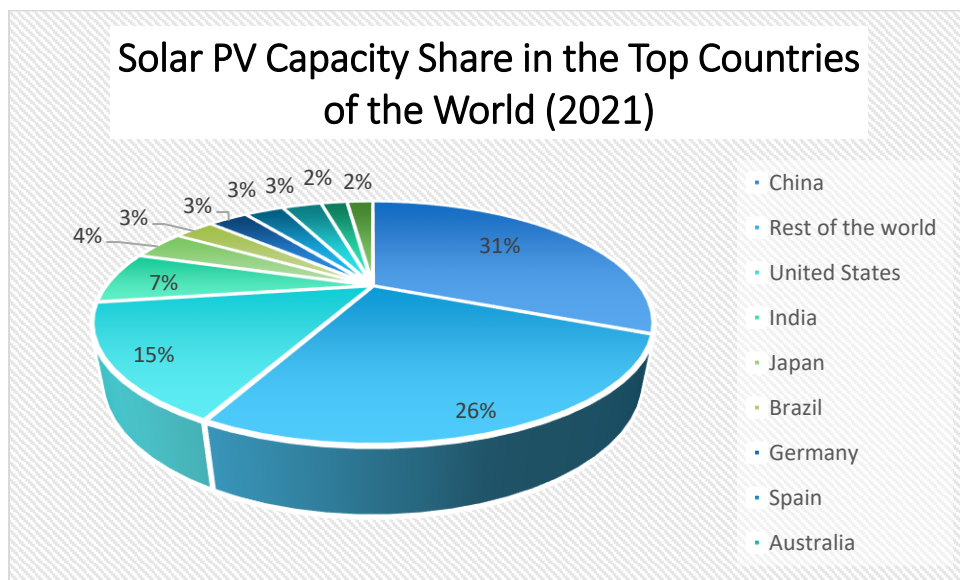


Figure 1.2 Solar PV Global Capacity Shares of Top Countries and Rest of World, 2021 [2]

Solar photovoltaic (PV) projects encompass various types that range from commercial, especially mega-scale projects, industrial, residential, micro-projects, and integrated PV projects. Integrated PV projects include road-integrated PV (RIPV), vehicle-integrated PV (VIPV), and building-integrated PV (BIPV), which are designed for specific applications with unique characteristics that match their specific conditions.

Solar modules are characterized by their low maintenance cost, especially those with fixed PV module types, as they do not have any moving parts. These modules are highly reliable, with a service life of more than 25 years, guaranteeing continuous electricity production. However, regular cleaning is required to limit any losses caused by soiling or dirt. The reliance of solar electricity on the sun as a fuel source eliminates the need to drill for petroleum-based fuels, refine them, burn them, or deliver them to the site. As can be observed, solar energy offers numerous advantages.

1.1.2 Road Integrated Photovoltaic

There is an increasing interest toward the integrated photovoltaic (PV) applications in the world. Examples of integrated applications are Building Integrated PV (BIPV), and Vehicle Integrated PV (VIPV) [3]. One of the most challenging integrated PV applications is Road Integrated PV (RIPV). For RIPV the solar cells need to be integrated in the road surface such that the cells do not break under the mechanical loads exerted by traffic, and the road surface must be transparent enough for sufficient PV energy yield.

In addition, there are many requirements to use RIPV as road, such as durability and safety to be able to stand under all weather conditions of the road surface [4]. Various concepts for RIPV have been demonstrated with varying degrees of success. However, so far, the results are still far from warranting a large-scale application of RIPV.

Since most roadways are exposed to sunlight, the harvesting of the of the solar energy has high degree of matching to the road network specially the

photovoltaic one, the concept of the RIPV is emerging to modify the PV panels to be part from the road structure. The concept of the RIPV first introduced in 2009 [4], then related researches has rapidly developed in several years.

All the RIPV is designed in the form of modularity it's basic structure can be divided into three main layers from top to bottom as in Fig1.3 the first part is the transparent layer, the second one is the middle functional layer, the third one is the bottom protective layer usually consists of surface course, base course, and soil base course.

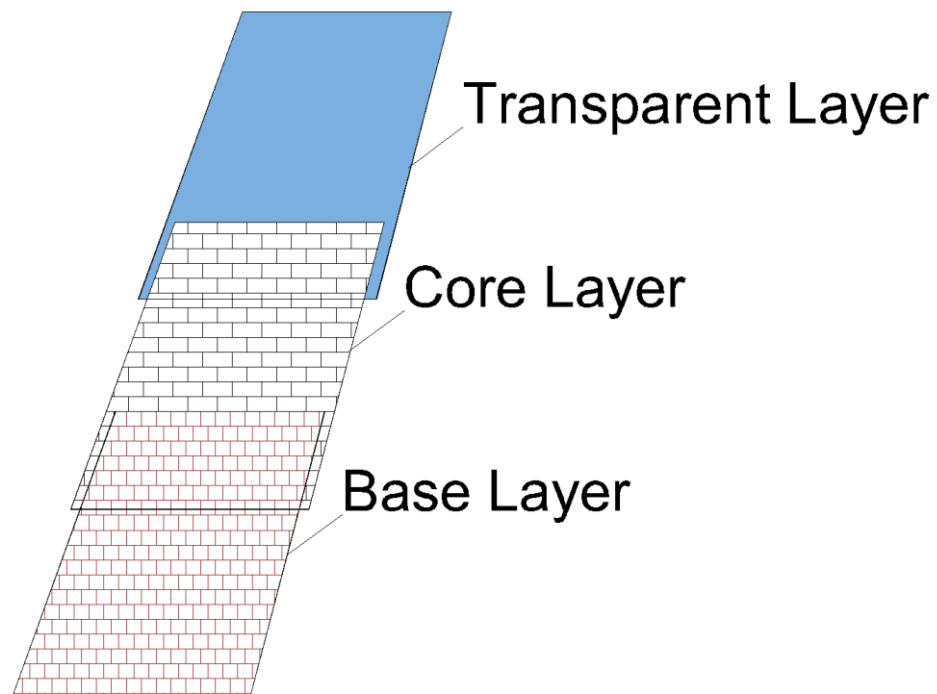


Figure 1.3 The basic construction of the RIPV modules. (Ref)

The transparent layer should be strong enough for the mechanical properties on one hand, it needs huge compressive strength to protect the pavement from deformation. on the other hand, should be equipped with reasonable anti-slip strength to ensure the safety of walking and driving, also it's the window for the solar irradiance for the coming sunlight it's better to have high transmittance index to avoid the power generation loss.

the materials applied on the surface transparent layer divided into three types: tempered glass, reinforced resins such as polymethyl methacrylate

(PMMA) ,and glass aggregate bonded by resins. Usually, its recommended to use tempered glass for the long-term stability than reinforced resins. The relatively poor skid resistance of glass could be improved by adding textures on its surface [4]

The central element of the intermediate functional layer is the solar cell, which can be either crystalline silicon solar cells or film solar cells. This layer is further categorized into solid and hollow models based on whether the surface layer is in direct contact with the solar cell. The hollow structure's surface layer is susceptible to damage due to uneven force distribution, potentially leading to moisture penetration. This moisture penetration poses a significant challenge, hastening the efficiency decline of the solar cell. Consequently, solid structures are predominantly employed in contemporary applications due to their resilience against these issues.[4].

The last layer major role is to transfer the loads from upper layer to the ground, protect the solar cells and other electronic devices from damage, seal pavement modules to avoid moisture penetration, tempered glass, concrete floor, resin and polymer substrate are all usual designs applied in the RIPV. The tempered glass is preferable and most applicable for its long-term stability and relatively light weight. The resin and polymer substrate made of waste and recycled material have ecological effects [4].

1.1.3 Partial Shading, Soiling Factor and Bypass Diodes

The outdoor performance of a PV module specially the RIPV is influenced by many factors. Some of these factors are related to the module itself and others are related to the location and environment. Few of these major factors are: material degradation, solar irradiance, thermal loss, ohmic resistances, fill-factor, shading, soiling, potential induced degradation, tilt-angle [5].

Light intensity is a very important factor in photovoltaic (PV) power generation, when the irradiance increases the current will increase, when there's reduce in the irradiance there will be greatly reduce in current also in generating power. That may happen due to the accidental factors some of the area of PV array will be shaded partly because of the obstacles such as birds,

street lights, trees, clouds, which will reduce the power and less the performance ratio (PR) for these PV's modules.

This common problem called the partial shading and considerably affects the power generated due to the voltage drop in the shaded PV cells. Other common causes for PV cells not receiving solar irradiance uniformly are dirt or soiling on the surface of the PV panels, Under such conditions, the PV modules area is partially shaded, leading to the occurrence of potential divergences in the generated current as we can see in Figure 1.4, the shaded module which connected in series will reduce the total current and start dissipating electrical energy in form of heat which in turn can cause hot spots, compromising the proper functioning of the PV system.

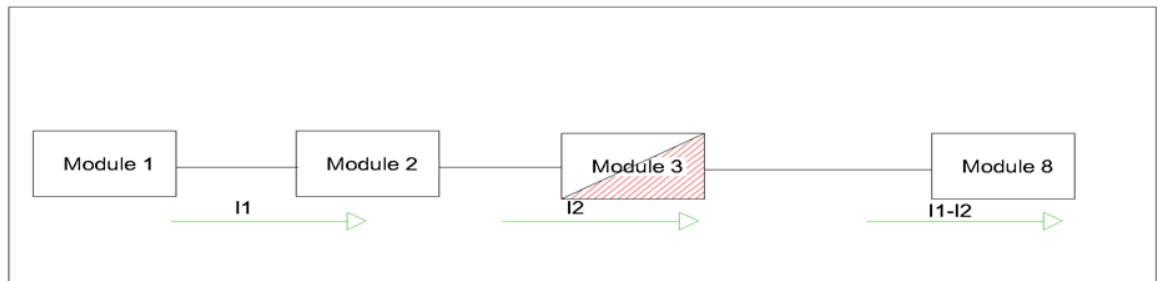


Figure 1.4 The systematic and current flow in series connected modules one of them is partially shaded.

To overcome this problem, which can lead to significant losses of generated PV power and even damage the PV modules, the most common practice is to install bypass diodes, in antiparallel with the PV module cells as we notice in Fig.1.5, aiming to bypass the current of the reverse polarized cells. Normally, the PV module cells are grouped according to the number of bypass diodes adopted by the manufacturer. Thus, it is possible to take one or more groups of PV cells out of operation, while the remaining continue to operate without any disturbance. So, it will let the current to enter in another pass when the cell is shaded (reverse biased).

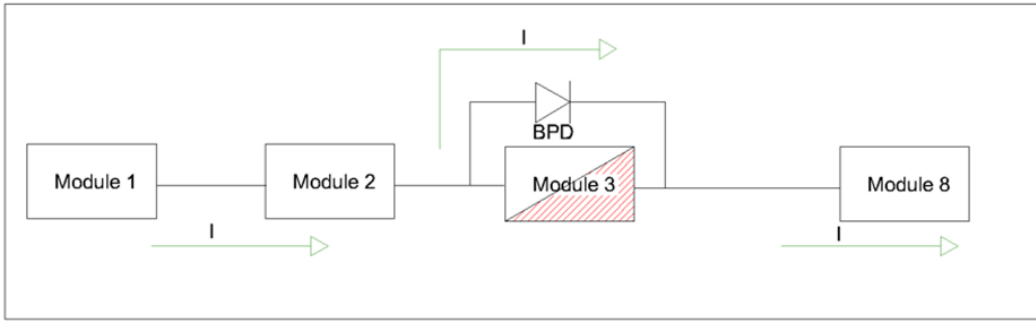


Figure 1.5 The impact of a bypass diode in the presence of partial shading on solar module

Fig.1.6 shows the Multi-level bypass diodes (MLBD) which can be added for group of cells in multilevel stages making different paths for the module current, when the cell is shaded the current path will be changed to pass through the bypass diode in order to keep the total current as it is and not be decreased, we can see there's different paths for the current the first and second one ,the difference between them is the voltage reverse bias, when there's two bypass diodes in the path the total voltage will be less ,and the losses of the power generated will be more.

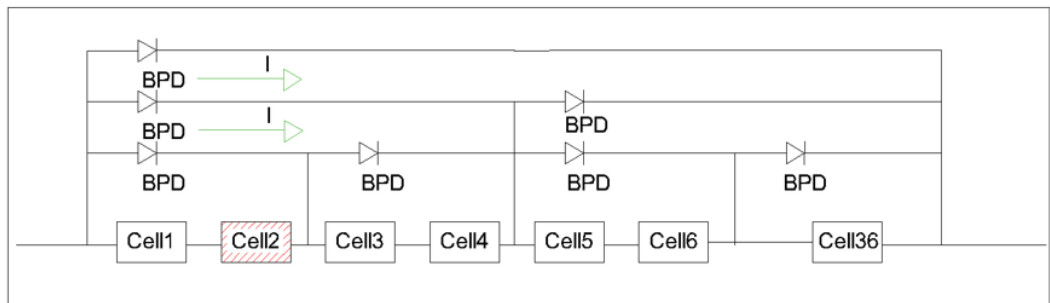


Figure 1.6 multi-level concept of Bypass diode in PV module cell

Soiling is the accumulation of dust, dirt, and other contaminants on a PV module. It leads to the formation of a thin layer over a module and thus reduces the light falling on one or many cells. Dust represents minute solid particles of diameter less than 500 μm [5]. Dust effect depends on factors such as dust properties (shape, size, weight), weather conditions (rain,

humidity, snow), location (coastal or dusty or in desert area), module tilt angle, surface finish and wind speed. Permanent soiling can occur if humidity condensate sticks dust to the surface, particularly for the tilted module that occur even after the cleaning operation for the panels, all dirt will settle on the bottom, but for the RIPV it will distribute on all the surface of the module without any concentration in a definite corner. Soiling in PV system may result into an annual power loss of 5-17% or more. Impacts of dust will be higher near highways and desert areas but will be less in areas with frequent rains and rural roads [5]. A rooftop PV system experiences fewer soiling losses as compared to a ground mounted system.

1.2 Problem Statement

The primary concern in this work lies in the challenges that confront the RIPV, which are concentrated in two principal factors. The first factor is the partial shading of the modules and strings due to the obstacles in their vicinity, such as trees, street lights, buildings, and other fixed shading elements. The second factor is the effect of soiling (dust), assumed to have large and small particles of dust will affect the PR for these PV modules and cause the losses that may occur under these conditions. These factors can negatively impact the PV performance ratio, and causes losses of the yield power and energy for the modules. To minimize the losses and optimize energy utilization and prevent the damage and hotspot issues, bypass diodes techniques will be added in parallel with the modules as a single stage or multi-level stages to make analysis and see how the performance before and after using the bypass diodes.

The results of this study will highlight the impact of both partial shading and soiling on cells and their effect on annual productivity, also the effect of adding bypass diode weather the single stage or the multi-level stage if it will contribute to reduce these losses and protect solar cells from hot spot issues.

1.3 Thesis Questions

The main question:

- What is the influence of both partial shading and soil on the productivity of RIPV solar cells, and what is the function of the bypass diode in reducing energy losses caused by these factors and protecting against hot spot issues?

Other questions:

- How the partial shading affects the modules and strings behavior of the RIPV?
- How is the yield energy of the different cases of the shaded parameters (Y_s), non-shaded parameters (Y_{ns}), homogenous parameters (Y_h) of RIPV?
- How to mitigate the partial shading losses of RIPV by the bypass diodes?
- How the soiling factor affect the PR and the energy yield of RIPV?
- What is the effect of using the single and MLBD on the dusty modules comparing the small particles and the large particles assumption?

1.4 Thesis Organization

This section is dedicated to providing a comprehensive overview of the thesis structure, facilitating seamless navigation throughout the entire document.

Chapter 1: General Introduction to Renewable Energy and PV Projects

Chapter 1 serves as an introductory foundation, offering insights into renewable energy and photovoltaic (PV) projects. Special emphasis is placed on Resilient and Intelligent Photovoltaic (RIPV) applications, delving into key challenges such as partial shading and the soiling effect. Additionally, the chapter explores the concept of bypass diodes. The subsequent section

involves an in-depth examination of relevant literature, encompassing various works and experiments in the field.

Chapter 2: RIPV Simulation Approach and Methodology

This chapter details the approach and methodology employed for the simulation of RIPV performance. The presentation commences by outlining the module locations and the topographical data surrounding the PV sites. Subsequently, irradiance and topography data are utilized to construct an irradiance model through the SSDP software tool. Spice simulation is then conducted, utilizing collected parameters from the PV modules to ascertain yield energy and power for eight modules. Two assumptions regarding soiling, based on dirt particles with (1 cm) and (5 cm) radius with 10% coverage fraction factor (CFF) from the module area, are introduced. The impact of these assumptions on yield energy is explored, with an additional examination of the influence of bypass diodes on performance.

Chapter 3: Discussion of Results

This one involves a detailed analysis and discussion of the results obtained from the output graphs and numerical data derived from the conducted tests and simulations. Special attention is given to elucidating the significance of incorporating bypass diodes in various scenarios involving solar modules, assessing the feasibility and benefits associated with their inclusion.

Chapter 4: Cost Analysis Chapter

In this chapter of the thesis, the primary focus lies on Bypass Diodes and Shade Tolerance within (RIPV) systems. Emphasizing the utmost importance of conducting a thorough cost analysis, this study serves as a crucial factor in determining the economic viability and practical feasibility of incorporating bypass diodes and shade tolerance features. Through a meticulous examination of associated costs, the research not only sheds light on the financial implications of adopting these technologies but also facilitates well-informed decision-making for stakeholders. The instrumental role of cost analysis extends to evaluating the return on investment, optimizing technology deployment, ensuring compliance with

financial regulations, and ultimately enhancing the overall success and market competitiveness of RIPV systems.

Chapter 5: Conclusions and Future Research

This chapter delivers conclusions related to the principal goals of the thesis, focusing on the efficacy of bypass diodes in alleviating power loss in Road Integrated Photovoltaic (RIPV) systems under partial shading. Furthermore, it offers suggestions for prospective scientific research initiatives within the domains of renewable energy, photovoltaic projects, and RIPV applications.

2 :Literature Review

2.1 RIPV

Since the RIPV project is totally recent, a few projects and experiments have been installed around the world, research operation is continuously to learn more and more about these projects to improve them. Nevertheless, the capacity to harness valuable energy from solar irradiation faces limitations imposed by the dispersed nature of available land. A strategic approach to address this constraint involves the utilization of roadways as a source for capturing incident solar energy. This approach allows for the optimization of land designated for transportation purposes [6]. Specifically, the adoption of Infrastructure Integrated PV (IIPV) technology to power the various loads associated with roadways offers the potential to minimize reliance on the grid. Additionally, employing IIPV can reduce distribution losses and alleviate the demand for copper, thereby yielding economic advantages [7]. Furthermore, IIPV has the potential to play a role in addressing challenges associated with extensive infrastructure upgrades in distribution grids, particularly in anticipation of heightened demand due to the widespread adoption of electric vehicles (EVs). Envisioning sustainable highways

involves the integration of high-powered solar road (SR) PV generation, wireless power transmission to EVs, and the implementation of self-healing asphalt[8]. This vision aims to establish a seamless transportation electrification technology.

Several researchers, including Sinan[4], have studied the development of projects related to solar roads. Sinan conducted a review of solar roads and discussed key RIPV projects implemented worldwide. In 2014, the SolarRoad pilot project was launched in Krommenie, Netherlands, marking the world's first integrated solar bike path. Initially, it measured 70 m in length and 3.5 m in width (refer to Fig 2.1). The path was constructed using prefabricated modules[9] that included top photovoltaic panels with an anti-slip glass coating and a bottom concrete baseplate. In 2016, the bike path was extended to 90 m, and the extension incorporated transparent resin with glass aggregate to enhance friction.



Figure 2.1 SolarRoad Project in Netherland.

Polycrystalline silicon comprising 80 wafer cells. These modules exhibit a rated output ranging between 293 to 313 Wp. The modules are interconnected into six parallel-operating grid-connected inverters through a dc/dc converter, activated if the predicted power surpasses multiples of an individual inverter's capacity [10].

The global irradiance at the installation location is determined considering the azimuth and altitude of the sun. The theoretical incoming irradiance, encompassing both direct and diffuse components, is computed for every minute throughout the year 2015. The direct irradiance is subject to variations based on distinct cloud cover and rainfall conditions, represented by the turbidity factor [11].

The research findings indicate that the module's peak estimated temperature and irradiance for January are lower than the measured values. In contrast, during June, the peak of the estimated temperature significantly exceeds the measured values. The second solar road project took place in France in 2016, conducted by Colas and INES, known as the Wattway project—the first solar road for vehicles in France. The road spanned approximately 1 km and comprised 2880 pavement panels. Fragile solar cells were coated in a transparent and resistant multilayer substrate made of resins and polymer, as depicted in Fig. 2.2. It's noteworthy that the energy output of this solar road has decreased over the years due to damage to the road surface. It's essential to acknowledge that all these projects experienced damage, emphasizing the need for further improvement and study in this evolving technology [12].



Figure 2.2 Wattway Project in France [5]

Some enterprises companies also launch some products of PV pavement. Such as Onyx in Spain and Solmove in Germany. Onyx developed a type of walkable PV paver for rooftop installation manufactured by amorphous silicon film solar cells and withstand up to 400 kg point loads [12]. Solmove

GmbH in Germany developed a type of PV pavement module with a self-clean profile that rainwater can drain well[13].

Evgenii [14] had an outstanding research on the VIPV which the PV modules are installed on the car's roof, sides, hoods or trunks. The captured solar energy then contributes the vehicle motion and reduces the frequency of the grid charging. Several commercial VIPV products already on the market such as "Toyota Prius PHEV", "Hyundai Sonata" they are examples of mass-produced vehicles with integrated PV modules. The main challenge in VIPV comes from the effect of local environment on module's performance specially the impact of partial shading.

Numerous methodologies for irradiance modeling have been put forth in preceding research [15] One such approach involves modeling solar irradiance through the random distribution of shading objects and subjects [16]. Another cohort employs the "Area Solar Radiation" function within the proprietary software ArcGIS to execute diverse computations related to VIPV[17]. DE Jong (year) have implemented an irradiance model based on the Perez All Weather sky model (AWSM) and digital surface topography data. They obtain hourly global horizontal irradiance (GHI) irradiance values from the nearest weather station and utilize sampled LiDAR data with a maximum resolution of $(0.5 * 0.5 \text{ m}^2)$ for topography data. Although their irradiance model bears similarity to ours, it is executed in MATLAB. Their data collection involves recording the PV module's voltage and current every 9.8 minute, along with location, orientation, ambient temperature, and wind speed.

Upon acquiring the irradiance data, it is necessary to model it using the SSDP library, which implements the Perez AWSM [18] This involves dividing the sky dome into patches and assigning irradiance values to each patch according to the Perez model. Additionally, the FreeSPA [19] library serves as an open-source implementation of the NERL solar position algorithm.



Figure 2.3 The RIPV pilot project Silicon Crystallin modules in Julich - Germany

In this research the irradiance model implemented similar to the one described in Fu and Rich [20] then modeled using SSDP tool, the data analysis and simulation models will be done on the RIPV modules from Solmove Germany company, they form small pilot project with capacity of (0.304 kWp), for research academic purpose as presented in Fig.2.3.

2.2 Partial shading, Soiling Effect and Bypass Diodes

Numerous studies have been conducted on the efficiency of PV systems, examining factors related to the PV modules, environmental elements (such as dust, soil, bird droppings, and snow), and surrounding structures that may cause partial or total shading. These factors contribute to inefficiencies in system performance. To address this issue, researchers aim to find methods to reduce partial shading losses [21] through the appropriate design of PV array configurations, Jazayeri [22] conducted a review of prior research in

this domain, identifying significant information and assessing the effectiveness of different photovoltaic array configurations under various shading patterns.

Fouad [23] talked about the main factors affecting the PR of the PV modules, they found that output power from PV panels is decreased due to the shadowing effect. Not only the shades affect the current flow in the shaded cells, but they also affect the whole current of that string since the cells are usually connected in series [23]. Several staff causing the shadow such as, trees, birds and buildings and may also be caused by the module mounting structures on other, if it's roof or ground tilted, leaves, birds and bird droppings that may fall directly on the modules can also cause shadowing. Several interconnection schemes are proposed to reduce the losses caused by partial shading. In one of the studies, Quaschnig & Hanitsch [24] showed that the performance loss was 70% although only 2% of the module area is shaded. Vittanen [25] concluded there's a 80 % loss if 5-10 % of the module area are shaded. Another study by Alonso-Garcia [26] stated that different power losses have been noticed with different configuration for the same amount of shadow, the amount of power loss will depend on the percentage of shaded cell and the material of the cell. The shades also depend on the height of the nearby buildings and the presence of trees or street lights, they stated the importance of using bypass diodes by analyzing the sub-curves models, statements regarding possible power losses at mismatched or shaded solar cells can be made. It's essential to minimize the power losses resulting from shading, and to avoid the damaging of the solar cells by hot spots during high power losses. The performance losses can be reduced using a bypass diode over every cell, even that's will not work if there's full shading over all the cells, because will have a high voltage drop, to reduce the power dissipation of a faulty cell it's better to increase the number of parallel connected cells than the series ones [27].

M.C. Alonso [26] stated that for the same cell shaded, the deformation of the module I-V curve increases with the amount of shading, moving the maximum power point to lower voltage values. Which mean losses in the power produced by the shaded cells will be different from the full shaded cell or the partially shaded cell, may reach 19% when half shaded, and 79% in the worst case when it's completely shaded.

Siyo Guo [28] had some experiments to model and study the PV module performance under moving shading with different configuration under partial shading condition of bypass diodes with the same modules at the same time. They found that the shadows that move in a certain direction horizontally or vertically, the bypass diodes configuration has a great influence than the number of bypass diodes used. Which should be taken into account while installing the PV modules.

Kim [29] had an experiment and simulations on two kinds of shaded cell, one with the bypass the other with MPPT controller, they found that bypass diodes are more effective to mitigate the hotspot for very short PV string length but not prevent the hotspot and damage to the PV cells, also the potential power that can be dissipated through a reverse-biased cell is lower than that with bypass diode, the hot spot issue occurs when the cell generates less current than the series connected cell in a string which leads to deformation of p-n junction, because of the dissipation of power as heat instead of producing power [30]. In addition to the conventional bypass diode technique which is effective in mitigation of the dissipated power from the hotspot issue [31], there are new techniques developed to prevent the hotspot issue such Active Bypass Switches or smart bypass diodes are an improvement over the bypass diode it reduces the voltage over the PV string and then the mitigation of the power will be less but do not resolve hot spotting, open-circuit the PV string or ensure that the cell can fully dissipate the worst-case power scenario without damaging the cell [32]. Photovoltaic Cells With Low Reverse-Breakdown Voltage which limit the power dissipated in during hot spotting may be an effective prevention method if dissipation at several times the rated maximum power can be managed without damaging the cell [29]. Further studies are needed to determine the susceptibility of cells with low reverse-breakdown voltage to hot spot damage, the last method is the Active Hot Spot Detection and Protection by monitoring and measuring the impedance [33] of PV shaded cells using algorithm with MPPT controller.

Ghazi [34] stated that dust on the surface of solar PV is widely distributed which settles on the surface of the solar module causing reduction in the system efficiency significantly. For example, in UK one of the cleanest region in the world, the dust effects reduce the solar irradiance by 5 – 6 %

after one month of not cleaning [15], the same result was concluded for a mono-crystalline panels after just one week in Israel done by Boykiw [35]. In contrast, in Sudan which has such desert region, the worst dust accumulation will decrease the solar irradiance by 40 % which is very big percent which effect the solar production [36]. Deposited particles and dust effect on the surface of PV panels is a complex phenomenon varying by climate, environment and location. A surface in a dry desert-like location is subject to electrostatically attracted inorganic materials while a surface in a coastal area is a subject to salts and rain driven dirt. Related experiments were done by Radziemska [37] in Poland to study the PR of the PV modules using artificially soiling dust produced impurities with grain 1 – 100 μm , 20 % with diameter 20 μm , 74 % were smaller grains, they concluded when the dust density from 0 to 22 g/m^2 the efficiency decreased by 26 %, Another test done in Libya by Mohammad et.al discovered that dust effect can cause reduction of 50 % in the panel output power [38], the last observation was done by Charabi et al. [39] in Oman and found that the dust will cause about 64 % reduction of the solar power which is the highest value at ever specially for the desert environment around.

Gostein [40] conducted experiments to monitor photovoltaic (PV) soiling losses, aiming to measure actual power output accurately. The soiling measurement stations employed in these experiments typically utilized a pair of PV modules, one of which was consistently cleaned, while the other was left to accumulate soiling at the natural rate. The output of each module was then compared to the reference device. When soiling is uniformly distributed across PV cells, measuring the short-circuit current followed by the output power proves effective. However, in practical scenarios, soiling accumulates on modules in a non-uniform [41] spatial manner, concentrating on specific areas such as the bottom or edges of the PV module.

Simulation of the current-voltage (I-V) curves for soiled modules using the LTspice circuit simulator revealed a non-uniform procedure in the I-V curve, resulting in a 9.6% reduction in maximum power. This underscores the importance of detecting non-uniform soiling in power measurements, as it significantly impacts the overall performance of PV modules.

Al-hasan [42] showed comparison of I–V characteristics for both clean and dusty PV modules for a sample of measurements, The open circuit voltage for both clean and dusty modules is approximately the same for the two modules. In contrast, the short circuit current and consequently the maximum output power decrease significantly for the dusty module. They concluded also as sand dust amounts deposited on the module surface increase more and more, the degradation decreases less sharply because the particles tend to accumulate on top of each other. A linear relation has been found to correlate the degradation in efficiency to the amount of sand dust accumulated on the module surface. Also, the decrease in PV module efficiency because of dust accumulation on module surface is estimated to be approximately equal to 33% for each 1 g/m² of sand dust accumulation.

Vidyanandan [5] stated, for the same dust type, smaller particles have greater impact than larger particles. This is due to the greater ability of smaller particles to reduce and block the light path more than that for larger particles this is for the tilted PV modules but in this research it's totally different because it's mounted horizontally on the road so the result is vice versa and the large particles will reduce the current in larger amount than the smaller ones. Power losses due to soiling of PV modules can be greatly reduced by regular cleaning. Many methods are available for PV cleaning including: manual washing, cleaning robot, self-cleaning glass, electrostatic curtain etc. The simplest among these is by regular wiping and cleaning with water. The frequency of cleaning will vary depending up on the location, season and module mounting. Soiling is a major factor for increasing Operations and Maintenance (O&M) expense of PV plants

Maghami [43] classified shading due to soiling in two categories: soft shading related to the environment and air pollution, which reduces the intensity of solar irradiance absorbed by the PV modules, that effect the current of the PV modules and the voltage remain constant. The second one is the hard shading, when dust accumulates and form clear particles on the surface of the modules that blocks the sunlight irradiance, then the performance of the PV module depends on whether some cells or all cells of the PV module are shaded. If some cells are shaded, then as long as the unshaded cells receive solar irradiance, there will be a current flow, in this

case there's high opportunity for occurring the hotspot issue for the shaded cell, which can be solved by the bypass diodes which causes decrease in the output voltage and the current remains constant of the PV module. The worst case when all the cells are shaded that's mean no power will be delivered in the PV module.

Fouad [23] stated the relationship between the losses from PV power and the soiling mass has deeply investigated and showed a linear proportional relationship between the two variables. when new dust particles settle on the existing ones, the soil mass increases and thus the surface becomes heavily soiled but doesn't cause further obstruction of light. The relationship between the soiling mass and the losses from PV power is affected by the geographical location since different light transmission is affected by the different dusts. Since the large particles have smaller cross-sectional area to volume ratio compared to the fine particles, they obstruct less light. Moreover, the composition and shape of the dust particle affect the absorption and scattering characteristics of the particle.

Hai Jiang [44] had some laboratory experiments were conducted to study the impact of dust deposition on different types of PV modules. A test chamber was used to access a natural dust deposition process and a solar simulator system was utilized to simulate the sun irradiance, the effects of dust deposition density, the irradiance density and the surface material. They obtained the corresponding reduction of output efficiency grew from 0 to 26% when dust deposition density increased from 0 to 22 g /m². The reduction of efficiency has a linear relationship with the dust deposition density, and the difference caused by cell types was not obvious, also the reductions of output efficiency at lower and higher solar densities were obvious, the degradation of PV module was mostly affected by large particles. The surface material has a potential influence on the output efficiency reduction. The poly-crystalline silicon cell covered with epoxy surface accumulated more dust than other two cells with white glass surfaces, they concluded the composition and shape of the dust particle affect the absorption of the solar irradiance and affect the PR of the PV modules.

Arash Sayyah [45] stated that when the tilt angle for the PV modules is 0 which is horizontally installed, the entire surface of the panel faces upward.

Since gravitational settling is the primary mechanism for dust deposition, the dust accumulation rate is highest under this condition. The surface area of a solar collector projected upward decreases as the tilt angle increases from 0 to 90. When the PV module is positioned vertically, the primary deposition mechanism of soiling is the diffusion of particles. Since the gravitational soiling rate is proportional to the equivalent diameter of the particle, one can see that the larger the particle size, the higher the deposition.

Hanifi [46] conducted experiments and simulations on a 60-cell crystalline silicon photovoltaic (c-Si PV) module developed by AE Solar. The primary objective of these endeavors was to enhance the reliability, power output, and energy yield of photovoltaic modules, particularly under varying partial shading conditions. Departing from the conventional approach of incorporating one bypass diode for every 20-24 solar cells, the novel methodology involved the protection of each individual solar cell with a dedicated bypass diode. This strategic measure aimed to minimize power loss and reduce the probability of hot spots within the PV modules.

A comparative analysis was undertaken, pitting a standard module equipped with three bypass diodes for all cells against a specially fabricated hot-spot-free module featuring integrated bypass diodes for each individual cell. The shading experiment introduced diverse shading patterns of varying sizes and directions. This ranged from the partial to complete shading of a single solar cell to the shading of an entire row in portrait orientation, where every two neighboring solar cells were fully shaded. Subsequently, multiple rows were shaded to an extent equivalent to the length of six solar cells from the bottom to the top in portrait orientation. The shading process was systematically increased from 10% to 50% of the total module area[46].

The outcomes indicated that, in instances of shading affecting 5-6 cells, the standard module exhibited zero power output, whereas the hot-spot-free module experienced only a 7% reduction in its total power output. Remarkably, when two cells of each string were affected by shading indicative of complete shading of one row—the module demonstrated a mere 20% decline in its total power output. The study's conclusion highlighted that the hot-spot-free module, incorporating integrated bypass diodes for every single solar cell, significantly enhances module

performance under shading conditions. Across various shading scenarios, the module demonstrated an additional power output of up to 32% (single solar cell shading) and 80% (one-row shading) compared to a standard module. Notably, even when 50% of the total module area was shaded, the hot-spot-free module continued to produce 10% of its nominal power[46].

The present inquiry seeks to provide fundamental insights into the data analysis of Germany's inaugural RIPV solar project. It will undertake a thorough investigation into the impact of partial shading and soil conditions on the efficacy of photovoltaic cells. Additionally, the study will assess the effectiveness of the single stage and multi-level stages of bypass diodes in mitigating energy losses and safeguarding the cells against hot spot issues.

3 : Approach and methodology

Photovoltaic (PV) yield modeling and forecasting starts from modeling the irradiation. Especially for integrated Photovoltaic applications such as building-integrated PV (BIPV) or vehicle integrated PV (VIPV), but there are some restrictions sometimes such as complex sites shading condition that should be taken into consideration to avoid the shading effect as much as possible.

This study will focus on RIPV with capacity of (0.304 kWp) solar project, located in the Julich research center campus in Germany. It will investigate the partial shading and the soiling effects on these modules. Finally, the research will study the impact of adding bypass diodes with different configurations, to the simulation of the RIPV; where the weather data, irradiance data, electrical data and topography for these modules are needed.

3.1 RIPV Performance Simulation

The inquiry will be on the Solmove RIPV which is one of the smart street PV panels manufactured in Germany. It is installed in front of the Photovoltaic and Climate building road in Julich research center. The system can be seen in Fig.3.3 where the RIPV silicon wafer is located, it contains 8 modules, ($60 \times 60 \text{ cm}^2$), each module includes 36 cells connected in series as illustrated in Fig.3.1 and Fig.3.2.

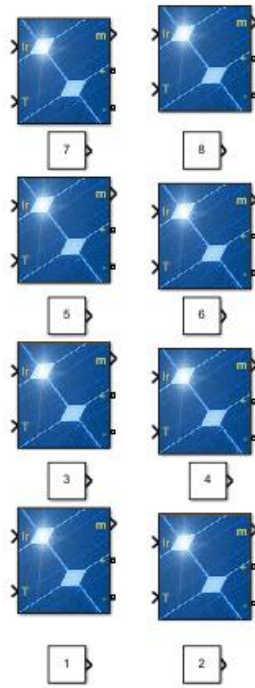
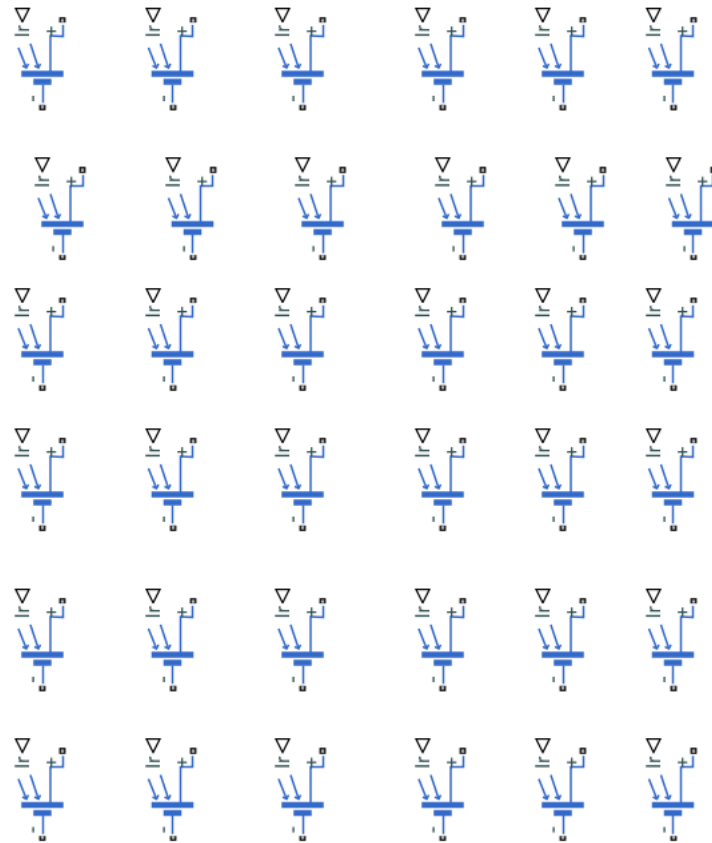


Figure 3.1 The series connection between solmove (8) modules



Cells Arrangement
(36) series cells

Figure 3.2 The (36) series connected cell for each module



Figure 3.3 Silicon Wafer RIPV with capacity (0.304 kWp) ,Solmove (38 wp),8 modules installed

The top transparent layer is to let the solar irradiance fall on the solar cells, was made from glass tape material with paving slab layer for safety, the core layer was made of silicon wafer crystalline then insulated by bitumen adhesive as back glass. The bottom layer was made of the compressed sand with gravel, frost protection as can see in Fig.3.4, it's from Solmove modules company located in Germany.

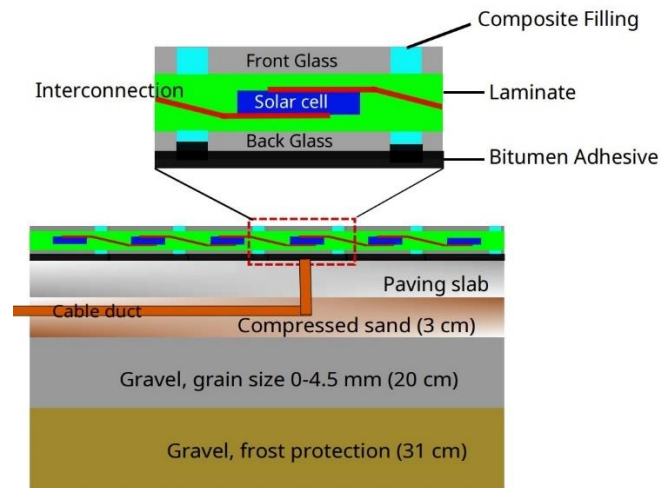


Figure 3.4 The structure of the RIPV modules project in Julich

By the current technology development, more and more Digital Elevation Model (DEM) data becomes available. It allows for a detailed description of the local shading conditions. For example, high-resolution light detection and ranging (LiDAR) data sets are freely available for North-Rhine Westphalia in Germany and the complete Netherlands. For the topography data it was used sampled LiDAR data with maximum statistic with resolution is about (0.5×0.5) m² which helps to determine the exact coordinates for the site and the complete map plot for the modules and the buildings, trees, roads as appears in Fig 3.5 showing all the site conditions around the RIPV.

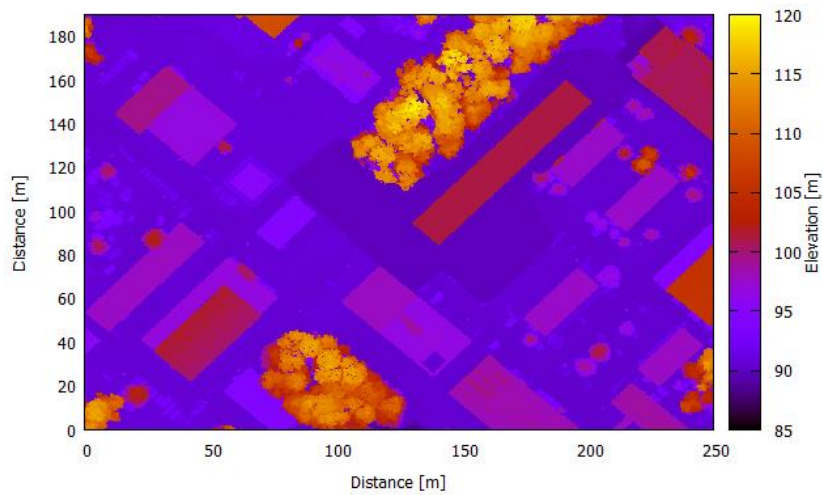


Figure 3.5 Topography for the RIPV and the staff around, in the Julich research center campus

Using the irradiance data and the topography data, Fig 3.6 shows a very high-resolution image that was implemented to show sunny moment taken afternoon on 15/June/2015, clear sky day, the maximum GHI value in the year in Germany - Julich is about 1400 w /m². It shows as well the shading site condition from the shading objects like trees, buildings around the red squares which represent the RIPV modules.

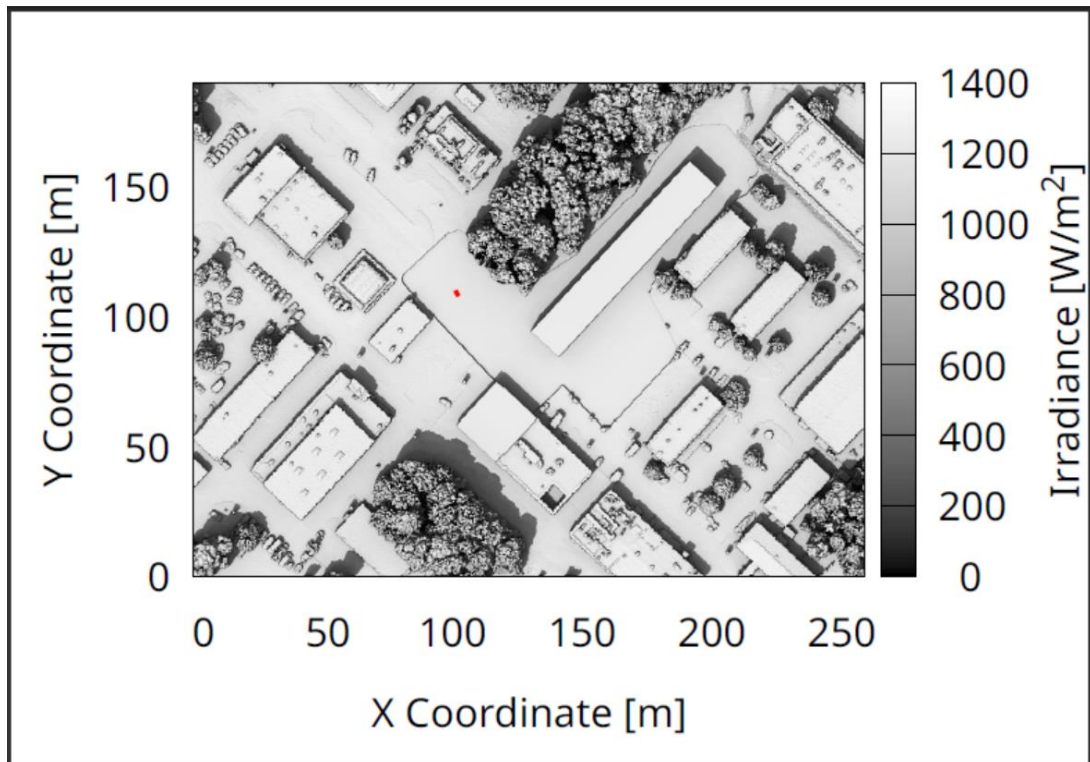


Figure 3.6 The image of Irradiance and shading for the staff around with high resolution, the red square presents the RIPV modules

Various tools have been developed to model the solar irradiation resources like r.sun [47], Solar Analyst [48], the commercial software PV*SOL [49] and PV*Syst software. However, for our purposes, most of these solutions have several shortcomings. Firstly, many freely available solutions have been designed to model the irradiance on a large grid. This large grid approach may have many applications, for VIPV, where the needed irradiance is only along a specific route having only one location per time step. This leads to a considerable overhead. Furthermore, most solutions are used of an isotropic sky approximation for the diffuse irradiance components. When used with diffused light, it becomes non-isotropic under many weather conditions.

The validation process for model implementations in SSDP consists of two steps. Initially, validate the AWSM and sky dome implementations. For this purpose, then utilize experimental data obtained from a field installation for GHI, DHI, and POA irradiance. SSDP implements the Perez AWSM[18] in a variable sized sky-dome mesh, this model depends on GHI and diffuse horizontal irradiance (DHI). When the GHI equals DHI the sky is completely cloudy, when the GHI is much bigger

than DHI, the sky is clear. A DEM may either be defined on a regular rectangular grid, or on an unstructured mesh. Various simulation modes make SSDP suitable for both; fixed PV installations and VIPV applications. As we see in Fig.3.7 SSDP model measures the time, coordinates for the place, then computes the sun location and the earth distance, then computes GHI and DHI values.

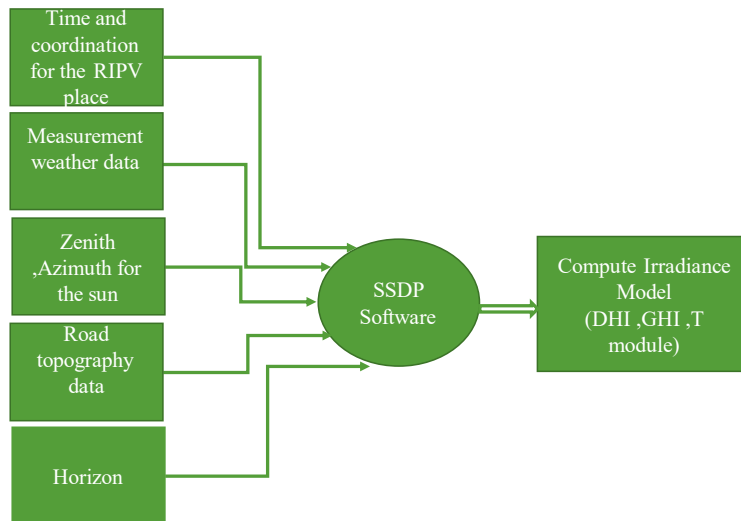


Figure 3.7 PV Irradiance Modeling using SSDP software taking into account the DEM.

The irradiance model takes the data for all the year 2015 as an input, matrix with every 5 minutes resolution, (5*5 cm²) grid with 25 irradiance value for each cell then takes the average value for the cell irradiance, all the parameters were collected from the weather station of the RIPV, the site condition shading data was collected using LiDAR data which is affordable freely in the North Rhyne in Germany as we can see in Fig 3.8.

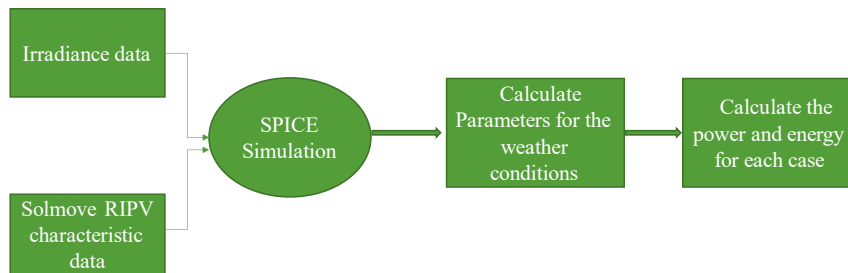


Figure 3.8 SPICE model simulation inputs and outputs implementation

This research is especially interested in investigating the different RIPV concepts with respect to shading losses. For the shading losses we need to distinguish between shades from the environment (trees, buildings, street lights), from traffic, and from soiling. In general, the energy yield decreases dramatically under partial shading conditions. For this reason, part of the demonstrator is planned with a special electrical design to mitigate these losses. There will be (8) series modules, each one consists of (36) series cells, using different techniques and equations such as SSDP. It Computes sky domes according to the Perez AWSM and can project this sky on a tilted surface. The solar position is computed from longitude, latitude, date/time, air temperature and pressure, according to the Solar Position Algorithm (SPA). For SPA one can use the free spa package [50] . It can process topological data and compute a horizon and thus take into account shading. The SSDP program implements a basic syntax to compute parameters. It will compute all the irradiance Plane of Array (POA) for the shaded modules by subtracting the DHI from the GHI, then the photocurrent for each cell can be calculated according to the Standard Test Condition (STC) of the cell as shown in equation 4, and compared to the average homogenous irradiance distributed over the modules, the difference between the shaded values and the homogenous will give the mismatch loss for those modules, also the

irradiance model for the unshaded modules was calculated considering POA is equal to the GHI, using this method the shading loss could be configured.

3.2 SPICE Simulation and Modeling of Bypass Diodes to Mitigate Partial Shading Effect

The investigation pertained to the RIPV Solmove crystalline wafer Cells, with their corresponding characteristics outlined in Table 3.1. A Simulation Program with Integrated Circuit Emphasis (SPICE) model serves as a mathematical portrayal of an electronic component or circuit employed within the SPICE software. Its primary purpose encompasses the design and optimization of diverse electronic circuits, encompassing amplifiers, filters, oscillators, diodes, and power supplies. Furthermore, the SPICE model facilitates the assessment of circuit performance under varying conditions and deviations, while also aiding in the identification of prospective design issues or constraints prior to the manufacturing phase.

The SPICE model in this study fit to lab data so all these measurements are taken from the lab experimental test model. The output file data from SSDP is a binary file has the information of the GHI, DHI, T module, every cell has irradiance value in a time instant. This way one can find the photocurrent for each cell, these data will be the input for the SPICE simulation

The electrical design optimization of the shade-tolerant RIPV system is achieved through the integration and modeling of the MLB concept, utilizing SPICE simulations. These simulations involve the implementation of various bypass diode configurations in the RIPV system, considering different shading conditions. The model parameters associated with these simulations are detailed in Table 3.2. By employing SPICE simulations and analyzing the performance of the RIPV system with different bypass diode configurations, the electrical design can be refined to enhance shade tolerance and overall system efficiency.

Table 3-1 The datasheet for the Solmove modules, Crystalline Wafer Silicon modules.

Characteristics	Value
V_{oc}	22.5 V
I_{sc}	2.09 A
P_{mpp}	37.8 w
V_{mpp}	18.9v
I_{mpp}	2 A

To simulate a solar cell in SPICE, you can use the diode equation, which describes the current-voltage (I-V) relationship of a diode, including a solar cell. The diode equation for a solar cell is typically given as:

$$I = I_{ph} - I_0 \left(\exp \left(\frac{qV}{NkT} \right) - 1 \right) - \frac{V}{R_s} + \frac{V_{oc}}{R_s} \quad (3.1)$$

Where:

- I is the cell current.
- I_{ph} is the photocurrent, which is the light-generated current.
- I_0 is the reverse saturation current.
- q is the elementary charge (1.602×10^{-19} C).
- V is the voltage across the solar cell.
- N is the ideality factor.
- k is the Boltzmann constant (8.617×10^{-5} eV/K).
- T is the absolute temperature.
- R_s is the series resistance.
- V_{oc} is the open-circuit voltage.
- R_{sh} is the shunt resistance.

Given the parameters in Table 3.2, the photocurrent (I_{ph}) needs to be considered separately based on the light conditions, the current was calculated using the values of irradiance with reference to the STC conditions:

$$G = \int G(X,Y)dx dy \quad (3.2)$$

$$I = 2.1 A @ 1000 w/m^2 \quad (3.3)$$

$$f = 2.1 /1000 \quad (3.4)$$

$$I_{ph} = G_{cell} * f \quad (3.5)$$

Where:

G cell: POA irradiance

When have the V, I for each cell then the mean power will be calculated for all the cells and the yield energy also using these equations:

$$P_{mean} = \frac{1}{N} \sum_i^N V_i * I_i \quad (3.6)$$

$$E = P_{mean} * t \quad (3.7)$$

Where:

- E is the energy yield (in watt-hours or kilowatt-hours),
- P_{mean} is the mean power output of the module (in watts or kilowatts),
- t is the time the module operates (in hours) over the year.

Table 3-2 Characteristic parameters used in the SPICE simulation model for the solar cell.

Abbreviation	Value	Parameter
I0	.728*10 ⁻⁹	Saturation current
N	1	Ideality factor
Rs	.015	Series resistor
Rsh	718.50	Shunt resistor
F	.002130	Conversion factor
Eg	1.1230	Bandgap

After the simulation is done from the SSDP software and got the POA irradiance model for the various weather conditions and shading, it has been used to calculate the parameters of the non-shaded case, shaded case and the homogenous as shown in the schematic diagram in Fig 3.9. The data was

entered to the SPICE simulation to be analyzed, study and compare the power and energy yields results. To reduce the losses due to the partial shading, typically use bypass diodes in many configurations, in this study many configuration designs were assumed for the single stage and the MLB diodes. By modelling the bypass diode circuits using ng-spice [51], defining the single stage and the multi-stage level of bypass diodes, to study there effect in the yield energy, and how could mitigate the partial shading losses.

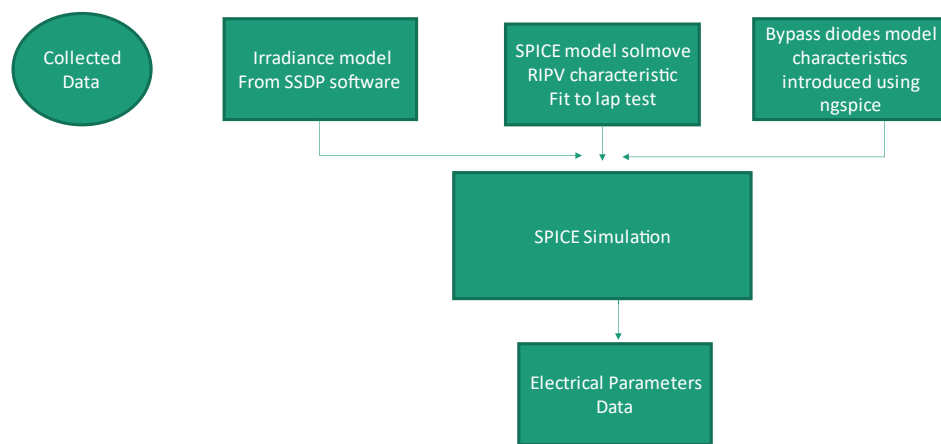


Figure 3.9 Schematic diagram of the collected data used in the SPICE simulation.

3.2.1 Concept and algorithm of Modelling MLB diodes:

In a PV module, individual solar cells are connected in series to achieve the desired voltage output. However, if one cell or a portion of the module in string is shaded or malfunctioning, it can significantly reduce the overall power output of the module. This occurs because shaded or faulty cells create a high resistance path, limiting the flow of current and affecting the performance of the entire module. To mitigate this issue, MLB diodes are integrated into PV modules. These diodes act as bypass switches, providing an alternative current path when shading or a partial failure occurs. When the voltage across a shaded or faulty cell drops below a certain threshold, the

MLB diode becomes forward-biased, effectively bypassing the shaded or faulty portion of the module. By redirecting the current flow, the MLB diode allows the remaining unshaded cells to continue producing power without being affected by the shaded or faulty cells. This helps optimize the overall power output of the PV module. In summary, the bypass concept of an MLB diode in a PV module involves redirecting current flow through an alternate path to bypass shaded or faulty cells, thereby minimizing power loss and optimizing the module's performance.

In this work the multilevel bypass diode concept was implemented using different configuration of bypass diodes designs which specified with a vector contain the number of bypass diode for each level for example $N_b = [3,9]$ makes two levels, the total number of cells are 36, the first level creates one bypass for substrings of $36/3 = 12$ cell, the second level makes one bypass for every $36/9 = 4$ cells.

3.3 Soiling Model

To examine the impact of soiling on the photocurrent of the RIPV, a soiling model was established. The model assumes the presence of both small and large particles distributed across the cells, resulting in approximately 365 distinct soiling patterns that are redistributed daily. Although this assumption may not reflect a realistic scenario, it serves as a basis for studying the effects on current and power generation. The aim is to evaluate whether the implementation of bypass diodes can mitigate and reduce these losses while safeguarding the RIPV system from potential damage.

The simulation script incorporates fixed average irradiance simulations and incorporates soiling distributions. Specifically, two scenarios were considered: one involving big particles measuring 5 cm with a dirt CFF of 10%, and another involving small particles measuring 1 cm with a dirt CFF of 10% of the panel area. These simulations enable the assessment of the generated current and power under these soiling conditions, providing insights into the potential benefits of employing bypass diodes in mitigating losses and preserving the performance of the RIPV system.

Figure 3.10 notifies the assumption of the small dirty particles of ($R=1$ cm), CFF of 10%, which presents the small soil or any other dirties which may stick to the RIPV, this was entered to the script to make the simulation firstly without BPD to study the losses power and their effect on the PR of the RIPV, then with the appearance of the MLBD in order to analyze and see how it could mitigate the losses and protect the RIPV's from hot spot issues.

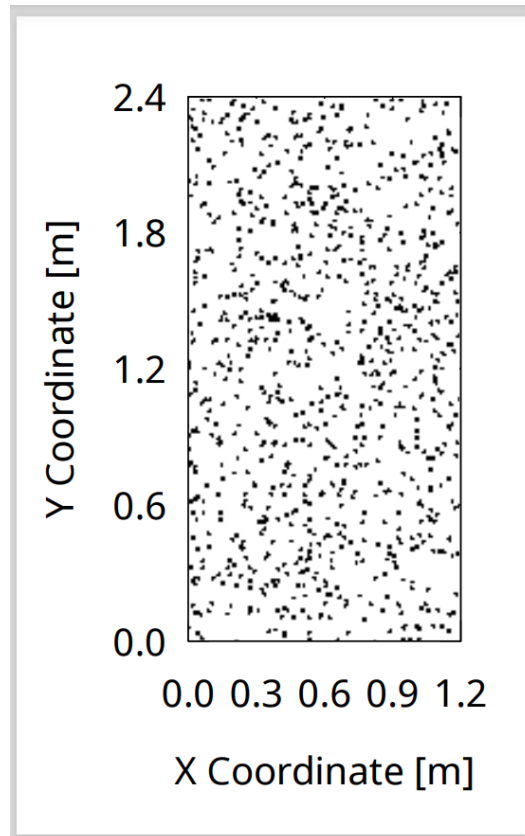


Figure 3.10 The assumption model of small particles of (1cm) radius distributed over the modules

In Fig.3.11 as the previous figure, it can be noticed that the assumption of the large dirty particles ($R=5$ cm), CFF of 10%, of the panel area which represents some leaves or any other dirties that may stick to the RIPV, this was entered to the script to make the simulation firstly without BPD then get the parameters to study the losses in power and their effect on the PR of the RIPV, then with the appearance of the BPD in order to analyze and see how it could mitigate the losses and protect the PV's from hot spot issues.

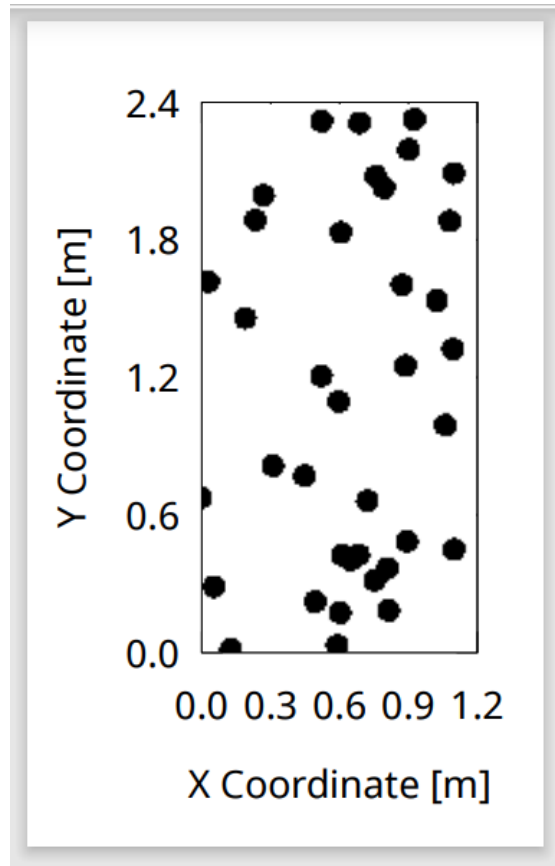


Figure 3.11 The assumption model of big particles ($R=5\text{cm}$), $\text{CFF} = 10\%$ distributed over the RIPV modules

4 : Results

In this section, will present the results of the data analysis for the RIPV performance. Additionally, will demonstrate the monthly power output in the presence of partial shading effects. The results will showcase the outcome of the simulation and modeling of MLB diodes considering two key factors: partial shading and soiling with various particle assumptions. Furthermore, we will thoroughly analyze and investigate these factors to gain deeper insights partial shading effect simulation on RIPV.

4.1 Partial Shading effect data analysis

As pointed out before in this research, the RIPV modules are surrounded with some shading objects and face partial shading issues which can't be prevented. This shading effect appears clearly in winter because the sun elevation is low so the shading will be the longest in November, December, January and February, below the data analysis simulation will be shown and discuss the PV performance and the yield power and energy after having the cells parameters of V & I according to equations (3.1) to (3.4), then calculating the power and energy yield according to equations (3.5) and (3.6).

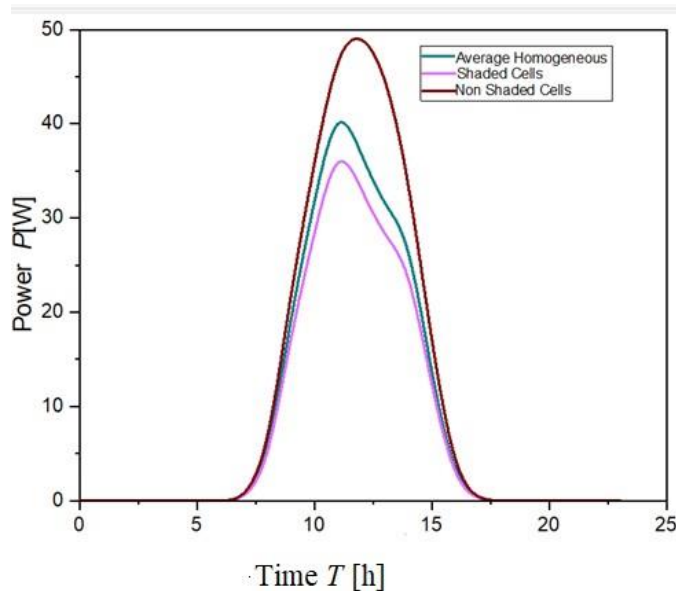


Figure 4.1 Partial Shading Effect in Power Generation for the Road Integrated Photovoltaic (RIPV) System during January 2015 for 8 Modules

In Fig. 4.1, it is observed that losses from partial shading in January significantly impact the period between 12:00 - 15:00 pm. This results in decreased power from the modules in both the shaded and homogeneous curves compared to the non-shaded curve. Additionally, the shaded curve exhibits greater losses than the homogeneous curve. The difference between them is attributed to mismatch losses, with power decreasing from 50 W to 40 W (amplitude) in the homogeneous case, representing a 20% loss. In the shaded case, power decreases from 50 W to 35 W, constituting 30% of the total power of the modules, indicating mismatch losses of about 10% for the RIPV.

Contrastingly, the best Performance Ratio (PR) for the modules was observed in June, approximately 177 Wp for the 8 modules, particularly when the irradiance values are optimal during this period, as depicted in Fig. 4.2. The homogeneous loss was 5%, while the shaded loss was 7%, resulting in 2% mismatch losses, the lowest value throughout the year.

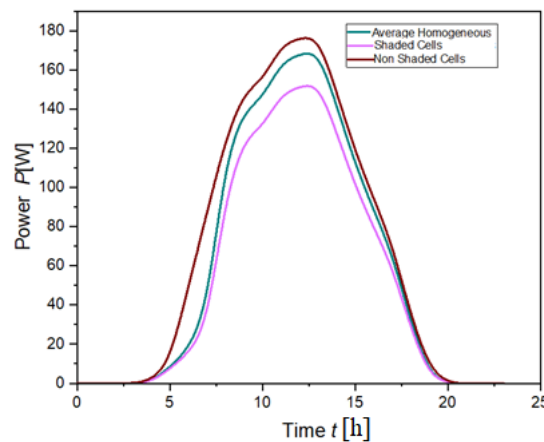


Figure 4.2 Optimal Output Power of the Road Integrated Photovoltaic (RIPV) System, Representing the Peak Productivity in June 2015 Using 8 Modules.

In Fig.4.3 it was noticed that the worst partial shading effect period in the year in Germany is in December. also noticed that the large decrease of the power between (11:00-15:30) pm, it decreases the power from 60 W to 40 W about 33 % decrease in the shaded case, and decreases in the homogenous case from 60 W to 44 W about 26 %, the mismatch loss is 7 % which is really a great issue should be solved.

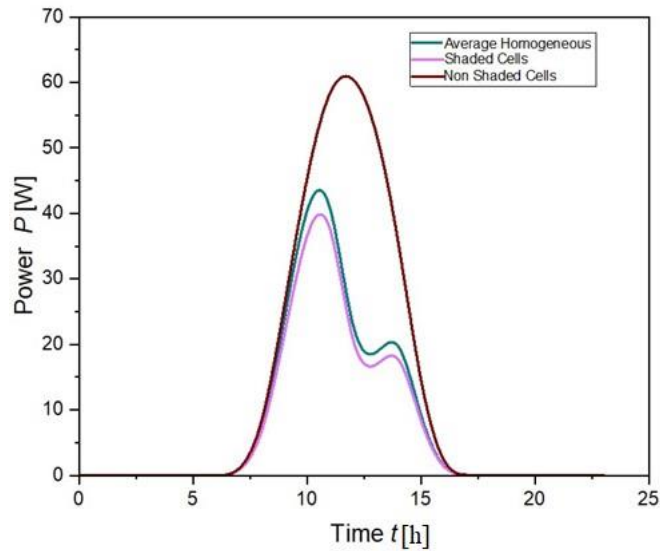


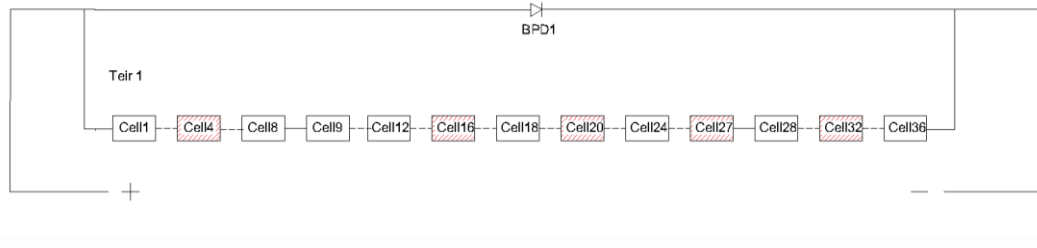
Figure 4.3 Partial Shading Impact on the Road Integrated Photovoltaic (RIPV) System in December 2015

4.2 Modeling and Simulation of adding MLBD Configuration:

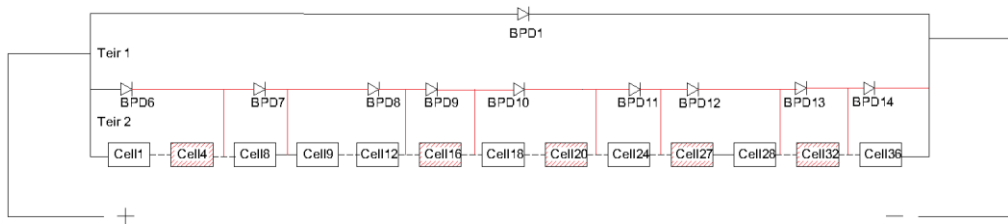
Trying to reduce the partial shading effect and protect from hotspot issues, the single stage bypass diode and the MLB diodes method will be used, the single stage was assumed having one diode, for the MLB diodes it was assumed to have many configurations designs:

- **Tier 1:** the first stage has 1 bypass diode for all the cells per module.
- **Tier 2:** that's mean it has 4 bypass diodes in the string, one per 9 cells
- **Tier 3:** the third one has 9 bypass diodes, one per 4 cells. As clarified in Fig.4.4
- ❖ Design A: Add tier 1 bypass diodes
- ❖ Design B: Add both tier 1,2 bypass diodes
- ❖ Design C: Add both tier 2,3 bypass diodes
- ❖ Design D: Add both tier 1,2 and 3

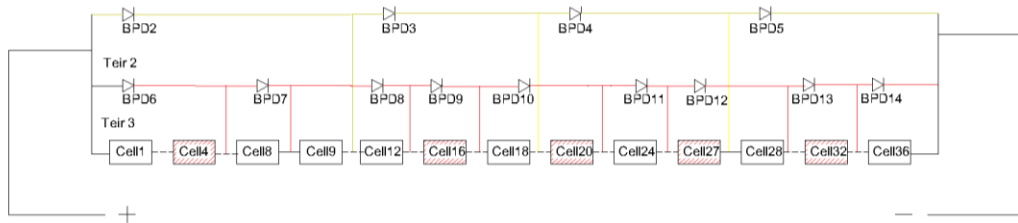
Design A



Design B



Design C



Design D

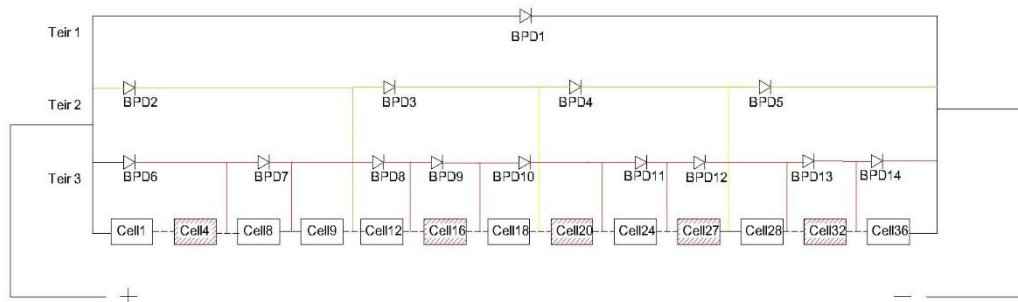


Figure 4.4 MLB diodes with varied configuration designs A, B, C, D consequently.

A previous observation highlighted the impact of partial shading on the total power generated by the modules. It was anticipated that the inclusion of MLBD would alleviate this loss to some extent. Based on SPICE

simulations, it can be deduced that the addition of MLBD does not significantly affect the partial shading as observed in Figure 4.5 as it shows the monthly power of February. The simulation results revealed the following optimal configurations arranged as follows: Design, A, B, C, D, also noticed from Figure 4.6 the energy yield over the year according to equation 6, it indicates the slight difference between the configuration designs of bypass diodes.

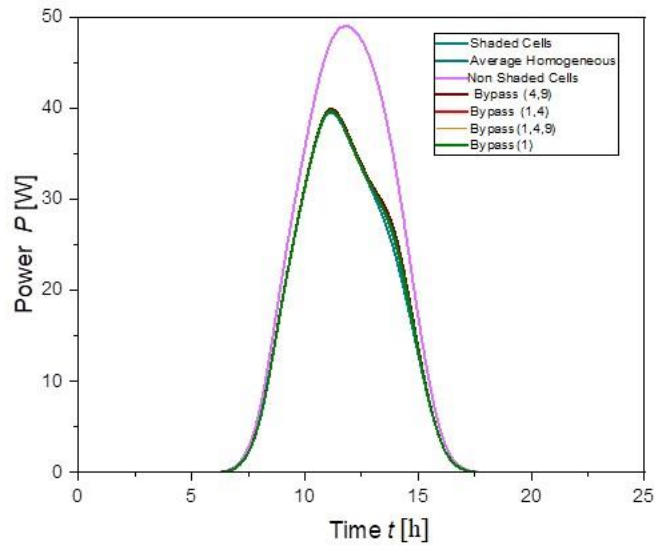


Figure 4.5 The Impact of Partial Shading in February Across Various Weather Models and the Influence of Incorporating Different Configuration Designs MLB diodes

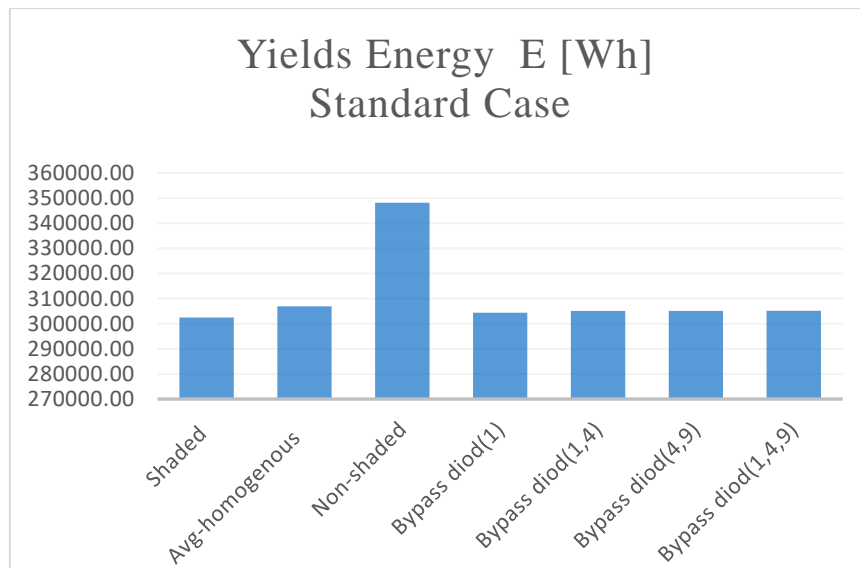


Figure 4.6 Annual Energy Yields Produced by All Modules Across Varied Weather Models, and with Diverse (MLB) Diode Configurations in Standard Conditions (Without Soiling Model).

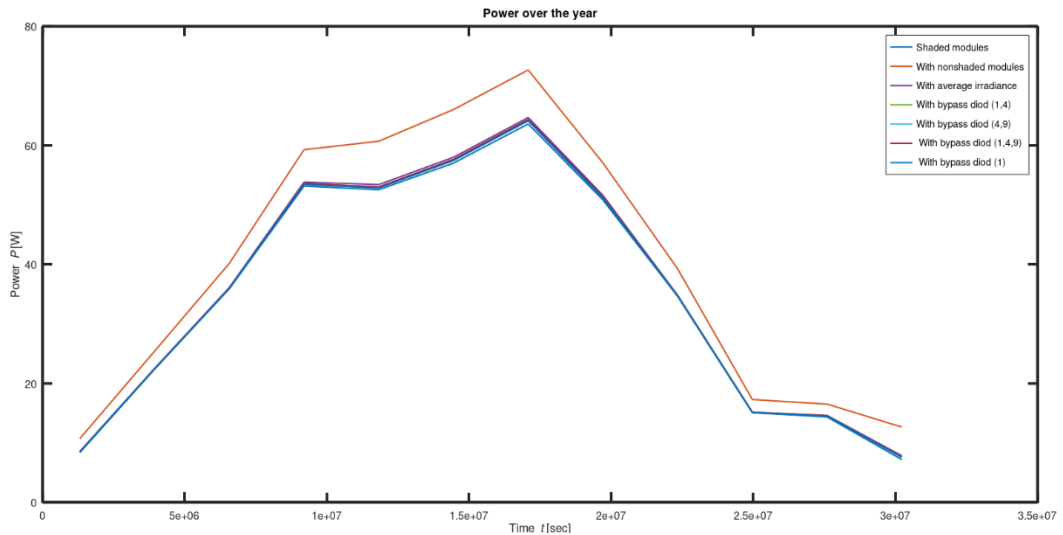


Figure 4.7 The Annual Power Generation for All Modules Across Varied Weather Models Under Standard Conditions (Excluding Soiling Model).

It's noticed from Fig.4.7 how is the power generated from the RIPV in all the modules all over the year (2015) specially it was recorded and collected by Julich center in high resolution, every 5 minutes. The best period for the production is at June, it has the best irradiance value, one can also see the best production curve when there's no shaded, the lowest one is the shaded modules, adding the MLB diodes could make small effect, the best energy yield was noticed as in Table.4.1 for the MLB diode design D (1,4,9).

Table 4-1 The Yield Energy yield for all the weather models and different configuration of MLB diodes for the 8 modules (Standard Case) without soiling factor.

Weather models & Configurations (Standard Case)	Energy yield (Wh)
Shaded, Ys	302,465.99
Avg-homogenous, Yh	306,930.90
Non-shaded, Y ns	348,168.39
Design A	304,391.80
Design B	305,059.55
Design C	305,079.01
Design D	305,173.08

As demonstrated earlier, the comprehensive shading loss, represented as $(1 - Y_s/Y_{ns})$, accounts for a substantial 13% of the total energy loss. Additionally, the mismatch loss, expressed as $(1 - Y_s/Y_h)$, contributes 1% to this loss, while the minimum shading loss, denoted as $(1 - Y_h/Y_{ns})$, stands at approximately 0.88%. These findings underscore the significant influence of shading effects on productivity losses.

4.3 Soiling Model and Simulation Result

To investigate the soiling factor impact on the RIPV (Photovoltaic System), two primary assumptions were simulated. The initial assumption involved the use of soiling particles with (1 cm) radius and a 10% CFF. The second assumption utilized soiling particles with (R=5 cm) radius, maintaining the same CFF.

Focusing on the first assumption, it was subjected to simulation, and the results were depicted in Fig. 4.8 and Fig. 4.9. These figures illustrate the power and energy yield generated by the 8 modules under various weather conditions and different configurations of MLB diodes, all based on the assumption of a (R=1 cm) soil radius pattern. Notably, the best performance was observed under non-shaded conditions, followed by homogeneous shading, and finally shaded conditions. Subsequently, there was a minor impact observed upon the addition of bypass diodes from the single stage to the MLB diodes configuration.

The summary of the energy yield was incorporated in Table 4.2, specifically in column 2. Adding a single bypass diode resulted in an additional energy gain of approximately 1,595 Wh compared to shaded yield production, which is equivalent to adding a new cell to the module.

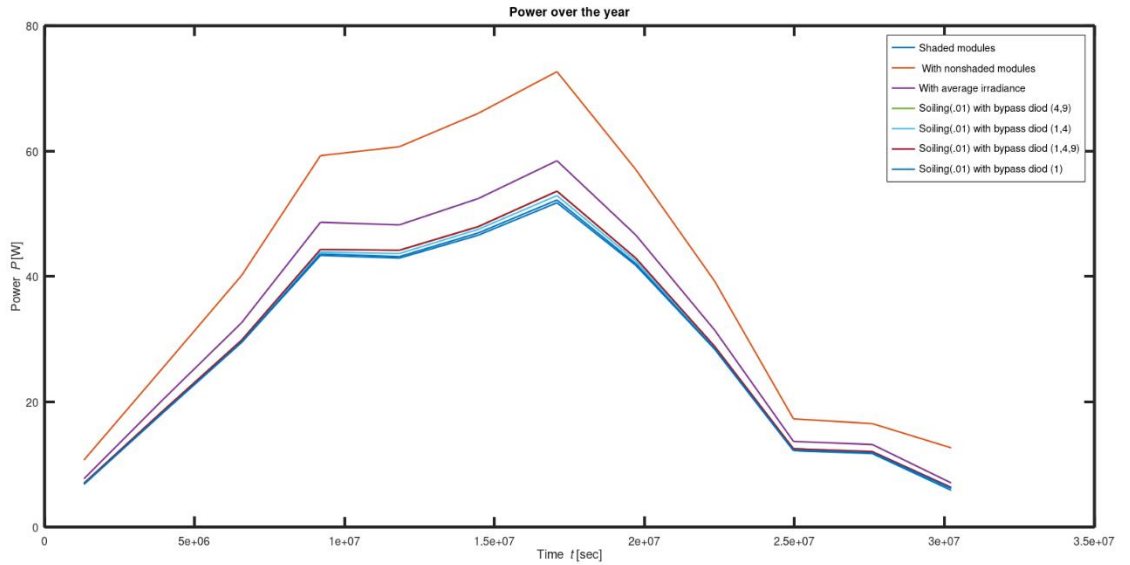


Figure 4.8 The Annual Power Generation for All Modules Across Various Weather Models and with diverse (MLB) Diode Configurations, Considering the Soiling Model Assumption (R=1 cm)

For the configuration MLB diodes B, adding the two level of the bypass diodes make a gain about (3,893 Wh) additional energy which is equivalent to adding new 3 cells to the module, the same to the C configuration, it makes a gain about (6,465 Wh) which equivalent to adding 5 cells to the module, then for the last configuration D, it makes a gain (6,538 Wh) which is equivalent to adding 5 additional cells to increase the yield production as shown in Table 4.3.

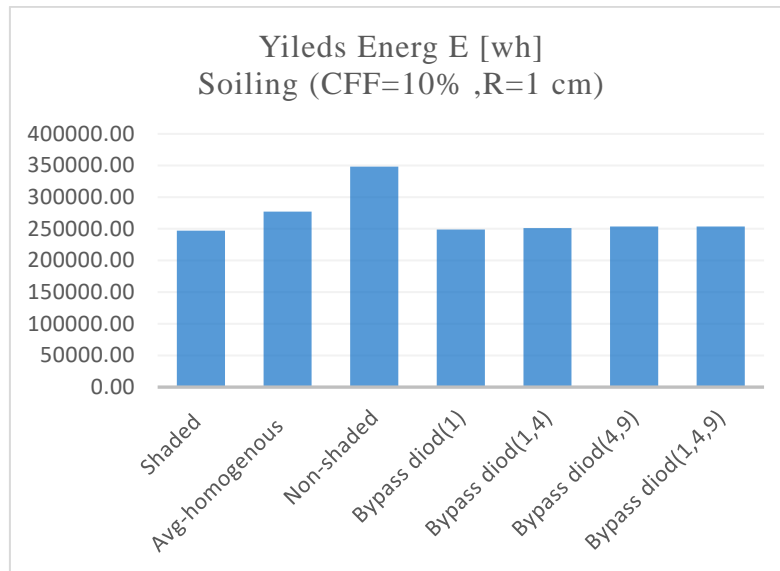


Figure 4.9 Energy Yield from All Modules Across Various Weather Models, and with Diverse (MLB) Diode Configurations, Incorporating the Soiling Model (1 cm)

The same thing was done for the second assumption for the large particles, from Fig. 4.10 and Fig. 4.11, it is evident that the shaded energy yield is significantly low in the case of dirty particles measuring 5 cm. This outcome contradicts the initial assumption of (1cm), which proposed that larger particles would cover multiple cells and result in complete shading, leading to power dissipation. Consequently, the distribution of power and current across cells would exhibit significant variations, causing a substantial loss of approximately 74% compared to the original assumption.

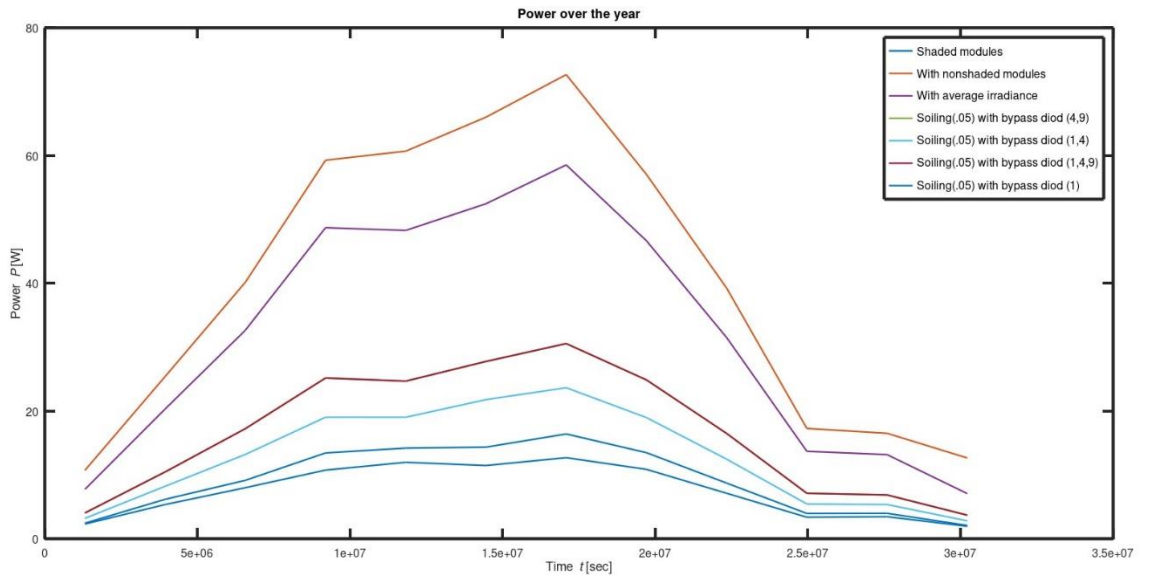


Figure 4.10 The Annual Power Generation for All Modules Across Various Weather Models, Considering the Soiling Model (5 cm) and (MLB) Diode Configurations.

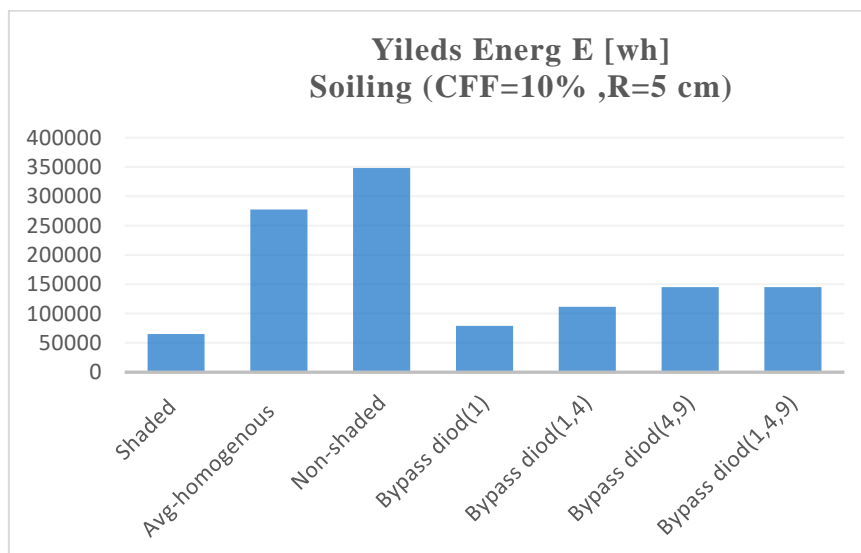


Figure 4.11 Energy Yields Generated by All Modules Across Various Weather Models, Incorporating Different (MLB) Diode Configurations, Considering the Soiling Model (5 cm)

While the realistic nature of (R=5 cm) distribution is debatable, it is important to acknowledge the inherent complexity of real-life scenarios. Although such losses are not commonplace, they can be observed in road applications that deviate from the norm. It is essential to consider the possibility of these significant losses when encountering highly non-uniform soiling patterns, particularly in poorly constructed roads with inadequate drainage or areas with a significant presence of fallen leaves from trees. This correlation aligns conceptually with the generation of soiling patterns.

As depicted in Table 4.2 and Table 4.3 By implementing the MLB diodes designs to the case of (R=5 cm) in column 4, configurations (A) adding the diode to each string, the energy yield increased by 21 % compared to the shaded energy yield. Design (B) which leads to increase by 72 %, the addition of two levels of bypass diodes results in an extra energy gain of approximately 46,519.59 Wh. This gain is equivalent to incorporating 38 new cells into the module. Similarly, for the (C) design configuration, the inclusion of MLB diodes leads to an increase in energy gain by 123 % of around 79,890.58 Wh, which corresponds to adding 66 cells to the module. Figure 4.12. shows the summarized yields energy generated from all the modules for the different weather models and different MLB diodes. Lastly, the (D) configuration, has again of 79,937.19 Wh, which can be considered equivalent to the addition of 66 extra cells to enhance overall production, yield gain for the soiling case (R=5 cm) shown in fig.4.12. Therefore, it is evident that incorporating MLBD aligns with the large particle assumption, as it yields massive improvement.

Table 4-2 The yield energy for the different weather models when adding the different design configuration of MLB diodes with soiling distribution of 10 % coverage fraction factor, and soiling R=1 cm ,5 cm Successively.

Weather models	Yield Energy (Wh)- Standard Case	Yield Energy (Wh) with soiling (CFF=% 10,R=1 cm)	Yield Energy (Wh) with soiling (CFF=% 10,R=5 cm)
Shaded	302,465.99	247,146.35	65,061.94
Avg-homogenous	306,930.90	277,229.66	277,544.02
Non-shaded	348,168.39	348,168.39	348,168.39
A	304,391.80	248,741.15	78,944.10
B	305,059.55	251,040.15	111,581.54
C	305,079.01	253,611.84	144,952.52
D	305,173.08	253,685.20	144,999.13

Table 4-3 The energy yield gain as a result of adding MLB diodes configuration designs.

Bypass configuration design	Gained yield energy (Wh) -Standard Case	Gained yield energy (Wh) - soiling (CFF=10%,R=1cm)	Gained yeild energy (Wh) - soiling (CFF=10% ,R=5cm)
A	1,925.81	1,594.80	13,882.16
B	2,593.56	3,893.80	46,519.59
C	2,613.02	6,465.49	79,890.58
D	2,707.09	6,538.85	79,937.19

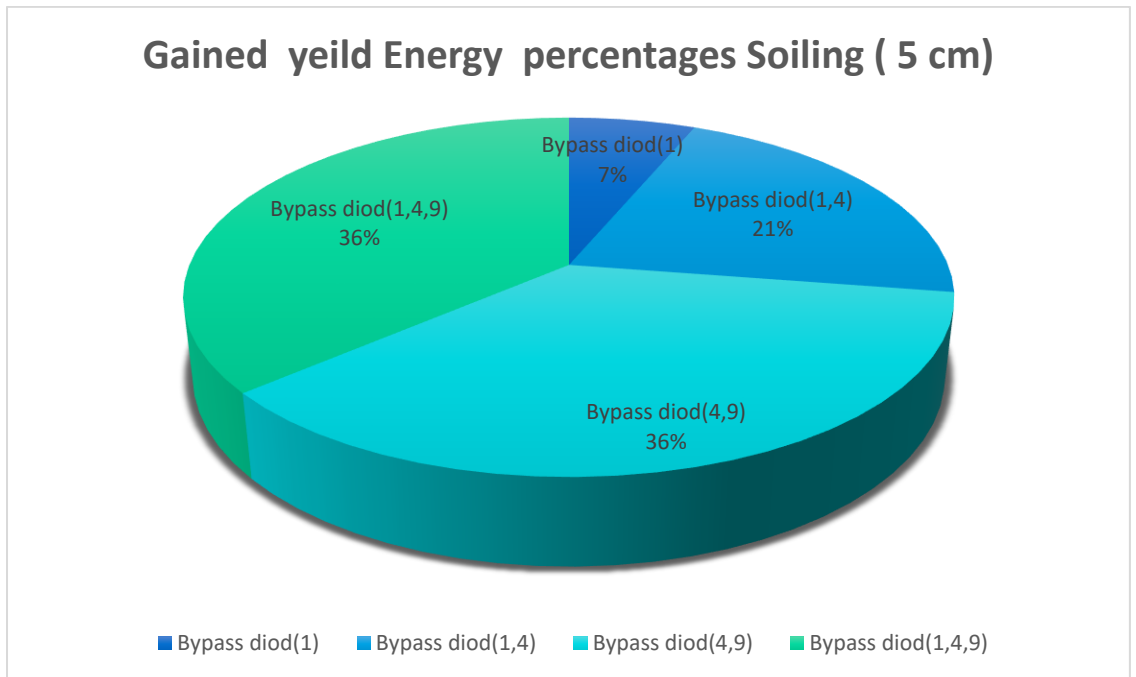


Figure 4.12 The acquired energy yield in the presence of soiling conditions (5 cm) was assessed by introducing distinct designs of MLB diodes denoted as A, B, C, and D.

4.4 Discussion of results

The shaded Road Integrated Photovoltaic (RIPV) has evidently influenced the PR and energy output, resulting in a 13% reduction compared to the unshaded cells. This substantial impact necessitates the exploration of mitigation strategies employing technologies such as bypass diode in one level bypass diode and the MLBD.

The energy yield for the different weather models using MLBD summarized in fig 4.13, By comparing the results of yield gains with the addition of bypass diodes relative the shading case, the addition of one-level bypass diode or MLBD configurations in both the standard case and the case involving soiling particles (R= 1cm and R= 5cm), the. The findings revealed an increase in yield production by approximately 0.63%, 0.65%, and 21.3% for Design A; 0.86%, 1.58%, and 71.5%, for Design B; 0.86%, 2.62%, and 122.8% for Design C; and 0.89%, 2.65%, and 122.9% for Design D. This signifies a noticeable enhancement in Design C and D, particularly in the

case of large particles ($R=5$ cm), warranting the inclusion of MLBD to mitigate significant power and energy loss compared to the shading case.

Furthermore, when comparing the increase in yield production with the addition of bypass diodes relative to the non-shading case, the corresponding improvements were approximately 87%, 71%, and 23% for Design A; 88%, 72%, and 32% for Design B; 88%, 73%, and 42% for Design C; and 88%, 73%, and 42% for Design D.

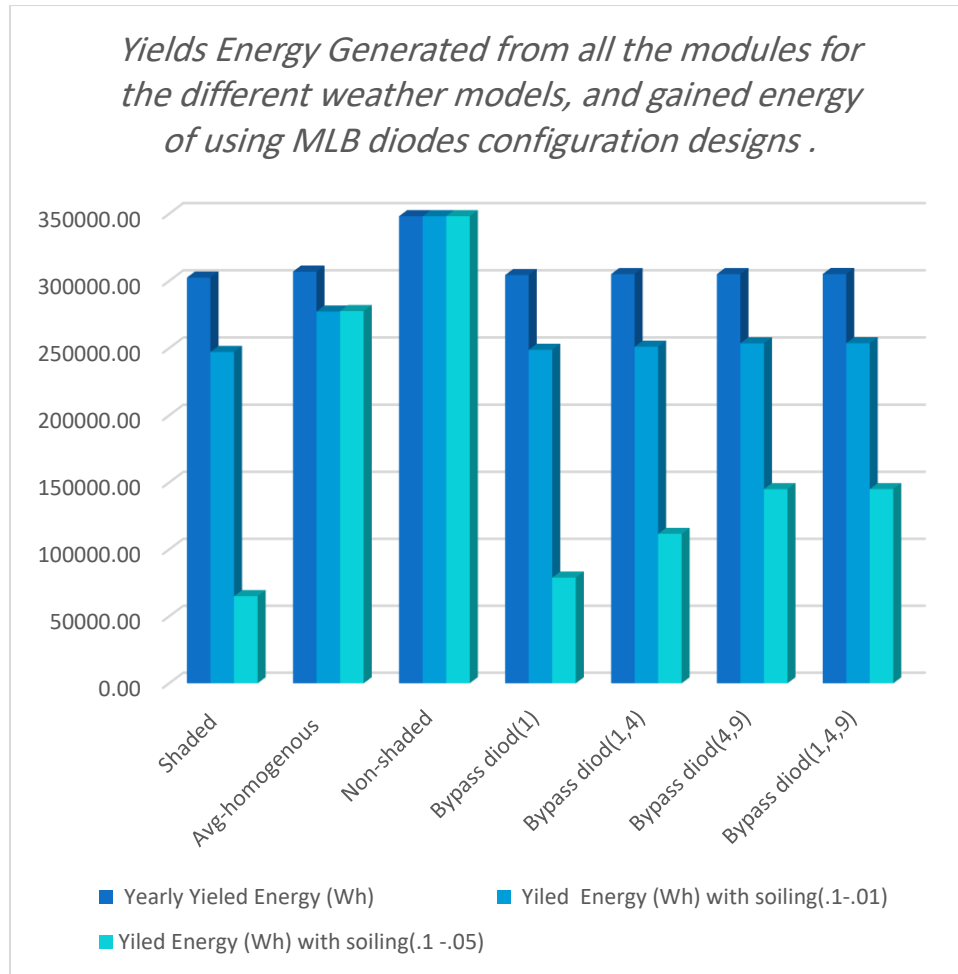


Figure 4.13 Yields Energy Generated from all the modules for the different weather models using MLB diodes configuration designs .

Based on the above observations, it can be concluded that the best effect of the MLBD in increasing the efficiency and productivity of the cells was achieved when it was in a state influenced by the soil coefficient of ($R=5$ cm), it was found that it significantly enhances their productivity and reduces energy loss, in contrast in the other two cases there's no significant effect on them.

5 : Cost Analysis

5.1 Introduction:

In the thesis study focused on Bypass Diodes and Shade Tolerance of Road Integrated Photovoltaic (RIPV) systems, conducting a comprehensive cost analysis is paramount. This analysis holds significant importance as it serves as a linchpin in determining the economic viability and practical feasibility of integrating bypass diodes and shade tolerance features. By meticulously assessing the associated costs, the research not only provides insights into the financial implications of implementing these technologies but also facilitates informed decision-making for stakeholders. The cost analysis is instrumental in evaluating the return on investment, optimizing technology deployment, ensuring compliance with financial regulations, and ultimately contributing to the overall success and market competitiveness of RIPV systems.

5.2 Cost Components:

The initial cost includes the solar panels, the inverter, AC & DC Cables and accessories, the bypass diodes and the installation cost.

5.3 Operational and Maintenance Costs:

The consistent operational and maintenance costs hold significant importance within the O&M plan. The routine adherence to and monitoring of systematic cleaning and maintenance procedures are essential, not only for managing labor salaries and maintenance tools but also for procuring spare parts as part of regular operations. This emphasizes the critical role that meticulous planning and execution of operational and maintenance activities play in ensuring the efficiency and longevity of the solar system.

5.4 Key Financial Metrics Analysis

Upon completion of the feasibility study for the three scenarios, the standard case (non-shaded), the soiling 5 cm, the soiling 5 cm with BPD, the outcomes have been consolidated and presented in the schedule below Table.5.1. This schedule serves as a comprehensive summary, encompassing key financial metrics such as the Payback Period, Net Present Value (NPV), Return Rate, Levelized Cost of Energy (LCoE), and Internal Rate of Return (IRR). These metrics collectively furnish a comprehensive evaluation of the project's economic viability and financial performance across the analyzed scenarios. The subsequent results and computations presented below are derived from the application of the following set of formulas and equations:

- 1) **Internal Rate of Return (IRR):** The IRR is the discount rate that makes the Net Present Value (NPV) of a project zero.

$$NPV = \sum_{t=0}^T \frac{CF_t}{(1+r)^t} = 0 \quad (5.1)$$

Where:

NPV = Net Present Value

T = total number of years

CF_t = Cash flow in period t

r = discount rate

- 2) **Net Present Value (NPV):** NPV is the difference between the present value of cash inflows and the present value of cash outflows over a period of time.

$$NPV = \sum_{t=0}^T \frac{CF_t}{(1+r)^t} \quad (5.2)$$

- 3) **Levelized Cost of Electricity (LCoE):** LCoE is the per-unit cost (usually per megawatt-hour) of building and operating a generating plant over an assumed financial life and duty cycle.

$$LCoE = \frac{\text{Total Cost}}{\text{Total Energy Output}} \quad (5.3)$$

- 4) **Payback Period:** Payback period is the time it takes for the initial investment in a project to be recovered through the project's cash inflows.

$$\text{Payback period} = \frac{\text{Initial Investment}}{\text{Annual Cash Flow}} \quad (5.4)$$

- 5) **Profit during 25 years:** The profit during 25 years would be the sum of the net cash flows over the 25-year period.

$$Profit = \sum_{t=0}^T CF_t \quad (5.5)$$

CF_t = Net cash flow in year t.

Table 5-1 Key parameters and financial metrics for three distinct scenarios of a solar project

Item	Standard Case (non-shading)	Soiling (R=5cm)CFF = 10 %	Soiling (R=5cm) with BPD, CFF=10%
Installed Capacity (kWp)	10	10	10
# of BPD	0	0	3696
# of modules	264		
Power of module(wp)	38		
Yearly (kWh/kWp)	1145	213	477
Initial cost of project (\$)	7000	7000	7500
LCoE(\$/kWh) for (1) kWp	0.1	0.5	0.24
IRR (%)	30.95%	-2.05%	9.15%
NPV return rate (\$)	12,939	-5,138	-491
Profit during 25 years (\$)	48,605	-1,743	12,088
Payback Period (Year)	3.2	36	10

The provided table presents a comparative analysis of three scenarios: Standard Case (non-shading), Soiling (5 cm), and Soiling (5 cm) with Bypass Diodes (BPD), each with an installed capacity of 10 kWp. The key

parameters and financial metrics for these scenarios are meticulously outlined. In the Standard Case, the system demonstrates optimal performance with an installed capacity of 10 kWp, resulting in a high Internal Rate of Return (IRR) of 30.95%, a positive Net Present Value (NPV) of \$ 12,939, and a relatively short Payback Period of 3.2 years. The Profit over 25 years and Levelized Cost of Energy (LCoE) are also favorable and cost effective one, reflecting the economic viability of the project.

Conversely, the Soiling (R=5 cm) scenario exhibits substantial challenges, with negative financial indicators such as an IRR of -2.05%, an NPV of -5,138, and a prolonged Payback Period of 36 years. The Profit over 25 years is notably negative, indicating significant financial losses. The LCoE is slightly higher compared to the Standard Case, contributing to the economic downturn.

The Soiling (5 cm) with BPD scenario addresses some issues by integrating Bypass Diodes, resulting in an improved IRR of 9.15% and a more favorable Payback Period of 10 years compared to the Soiling (5 cm) scenario. However, the NPV remains negative, suggesting ongoing financial challenges. The Profit over 25 years is positive but lower than the Standard Case, and the LCoE is slightly higher.

In summary, the comparison underscores the importance of shading mitigation measures such as Bypass Diodes, as they contribute to improved financial metrics and reduced Payback Period, mitigating the adverse effects of soiling on solar energy system performance.

6 : Conclusion and Recommendation

6.1 Conclusion

The results of this study focus on the performance coefficient and productivity of RIPV cells as one of the new applications for solar cells. It demonstrates the impact of partial shading as one of the challenges faced by this type of system. It also illustrates the effect of soil and dust on the productivity of these cells, two types of particles' size were assumed with ($R=1$ cm) and ($R=5$ cm) respectively with 10 % CFF. It is evident that there is a significant effect and energy loss in the second assumption, and the presence of the bypass diode will greatly improve the productivity of solar cells, equivalent to adding 66 cells to them which is economically viable.

The results of this study emphasis on the ability of adding MLBD in order to reduce the power and energy lost from the partial shading effect and the soiling factor in different scales, the highest effect was for the large assuming particles soil which related to the concept of the bypass diodes of finding new path for the current to decrease the losses as much as can. The study also reported the performance and the productivity of the RIPV as the first small project in Germany with capacity of (0.304 kWp) on Julich Research Center.

6.2 Recommendations

Based on the research results, the recommendations for solar cell manufacturers, particularly those producing integrated cells for use on the platform, include the following:

1. **Integration of Bypass Diodes:** Recommend the integration of bypass diodes as a standard feature in Road Integrated Photovoltaic (RIPV) systems. Highlight their effectiveness in mitigating the adverse effects of partial shading and soiling, thereby enhancing system performance and reliability.
2. **Optimization of Bypass Diode Placement:** Suggest further research or practical guidelines for optimizing the placement of Bypass diodes within RIPV installations. This could include recommendations for strategic positioning to maximize their impact on minimizing shading-induced losses.
3. **Development of Advanced Soiling Models:** Advocate for the development of advanced soiling models to improve the accuracy of predictions related to RIPV system performance. Emphasize the need for models that can account for various environmental conditions and provide more precise estimations.
4. **Continuous Monitoring and Maintenance Protocols:** Recommend the implementation of continuous monitoring systems for RIPV projects, coupled with proactive maintenance protocols. Regular inspections and cleaning routines can help prevent soiling effects and ensure the efficient operation of the system.
5. **Incorporation of MLB Diodes:** Depending on the findings, if MLB diodes were found to have a positive impact, recommend their incorporation as part of the standard configuration in RIPV systems. Discuss the benefits of MLB diodes in reducing electrical output disparities and enhancing overall system reliability.
6. **Education and Training:** Propose educational initiatives and training programs for technicians and installers involved in RIPV projects. This is to ensure that they are well-versed in the optimal use, maintenance, and troubleshooting of bypass diodes and other relevant components.

7. Future Research Directions:

- Suggest avenues for future research, particularly in areas such as advanced diode technologies, machine learning applications for soiling prediction, and real-world performance evaluations of RIPV systems with integrated bypass diodes, since the next part of this pilot project will be on the CIGS thin film solar cell with bypass diode for each cell,.
- Propose an investigation into the reliability of the Multi-Level Bypass Diodes (MLBD) and the potential repercussions in the event of a malfunction, as these diodes are susceptible to faults during operation. These recommendations collectively aim to guide industry practices, enhance system efficiency, and contribute to the ongoing development of sustainable and reliable Road Integrated Photovoltaic systems

References

- [1] Y. Hamakawa, “Background and Motivation for Thin-Film Solar-Cell Development,” pp. 1–14, 2004, doi: 10.1007/978-3-662-10549-8_1.
- [2] Solar Power EU, *Global Market Outlook For Solar Power FOCUS ON SOUTHEAST ASIA*. 2023. [Online]. Available: www.solarpowereurope.org
- [3] J. Markert, C. Kut

ter, B. Newman, P. Gebhardt, and M. Heinrich, “Proposal for a safety qualification program for vehicle-integrated PV modules,” *Sustain.*, vol. 13, no. 23, pp. 1–14, 2021, doi: 10.3390/su132313341.
- [4] S. Li, T. Ma, and D. Wang, “Photovoltaic pavement and solar road: A review and perspectives,” *Sustain. Energy Technol. Assessments*, vol. 55, no. November 2022, p. 102933, 2023, doi: 10.1016/j.seta.2022.102933.
- [5] V. K., “An Overview of Factors Affecting the Performance of Solar PV Systems,” *Energy Scan*, no. February, pp. 2–8, 2017, [Online]. Available: <https://www.researchgate.net/publication/319165448>
- [6] A. S. Dezfooli, F. M. Nejad, H. Zakeri, and S. Kazemifard, “Solar pavement: A new emerging technology,” *Sol. Energy*, vol. 149, pp. 272–284, 2017, doi: 10.1016/j.solener.2017.04.016.
- [7] M. S. Wu, H. H. Huang, B. J. Huang, C. W. Tang, and C. W. Cheng, “Economic feasibility of solar-powered led roadway lighting,” *Renew. Energy*, vol. 34, no. 8, pp. 1934–1938, 2009, doi: 10.1016/j.renene.2008.12.026.
- [8] P. Venugopal*, N. S. , A. Shekhar, E. Visser, and P. B. and S. S. G. Mouli, “Roadway to self-healing highways with integrated wireless electric vehicle charging and sustainable energy harvesting technologies,” *Appl. Energy*,

- vol. 212, pp. 1226–12, 2018, doi: 10.1016/j.apenergy.2017.12.108.
- [9] “SolarROad,” 2022. <https://www.solaroad.nl/>
- [10] N. N. A. Shekhar, V. Kumaravel, S. Klerks, S. Wit, P. Venugopal and M. Z. P. Bauer, O. Isabella, “Harvesting Roadway Solar Energy—Performance of the Installed Infrastructure Integrated PV Bike Path,” *IEEE J. PHOTOVOLTAICS 1*, vol. 8, pp. 1066–1073, 2018, doi: 10.1109/JPHOTOV.2018.2820998.
- [11] T. M. Kuchler, “Evaluation of models to predict insolation on tilted surfaces,” *Sol. Energy*, vol. 23, pp. 111–114, 1979.
- [12] Manhattan Penthouse, “Onyx, Solar Photovoltaic,” 2022. <https://onyxsolar.com/global-map/manhattan-penthouse>
- [13] GmbH, “Solmove,” 2018. <https://www.solmove.com/en/>
- [14] “Vehicle-Integrated Photovoltaics Irradiation Modeling Using Aerial-Based LIDAR Data and.pdf.”
- [15] S. Ghazi, K. Ip, and A. Sayigh, “Preliminary study of environmental solid particles on solar flat surfaces in the UK,” *Energy Procedia*, vol. 42, pp. 765–774, 2013, doi: 10.1016/j.egypro.2013.11.080.
- [16] M. Kolhe, S. K. Adhikari, and T. Muneer, “Parked electric car’s cabin heat management using photovoltaic powered ventilation system,” *Appl. Energy*, vol. 233–234, no. October 2018, pp. 403–411, 2019, doi: 10.1016/j.apenergy.2018.10.012.
- [17] T. Santos, N. Gomes, S. Freire, M. C. Brito, L. Santos, and J. A. Tenedório, “Applications of solar mapping in the urban environment,” *Appl. Geogr.*, vol. 51, pp. 48–57, 2014, doi: 10.1016/j.apgeog.2014.03.008.
- [18] R. Perez, R. Seals, and J. Michalsky, “All-weather model for sky luminance distribution-Preliminary configuration and validation,” *Sol. Energy*, vol. 50, no. 3, pp. 235–245, 1993, doi: 10.1016/0038-092X(93)90017-I.
- [19] FreeSPA, “Free implementation of NREL SPA,” 2022. <https://github.com/iek-5/freespa>
- [20] P. Fu and P. M. Rich, “Design and Implementation of the Solar Analyst: an

- ArcView Extension for Modeling Solar Radiation at Landscape Scales,” *19th Annu. ESRI User Conf.*, no. February, pp. 1–24, 1999.
- [21] K. N. Hajime Kawamura, Kazuhito Naka, Norihiro Yonekura, Sanshiro Yamanaka, Hideaki Kawamura, Hideyuki Ohno, “Simulation of I–V characteristics of a PV module with shaded PV cells,” doi: [https://doi.org/10.1016/S0927-0248\(02\)00134-4](https://doi.org/10.1016/S0927-0248(02)00134-4).
- [22] M. Jazayeri, S. Uysal, and K. Jazayeri, “A comparative study on different photovoltaic array topologies under partial shading conditions,” *Proc. IEEE Power Eng. Soc. Transm. Distrib. Conf.*, 2014, doi: 10.1109/tdc.2014.6863384.
- [23] M. M. Fouad, L. A. Shihata, and E. S. I. Morgan, “An integrated review of factors influencing the performance of photovoltaic panels,” *Renew. Sustain. Energy Rev.*, vol. 80, no. July 2016, pp. 1499–1511, 2017, doi: 10.1016/j.rser.2017.05.141.
- [24] V. Quaschnig and R. Hanitsch, “Numerical simulation of current-voltage characteristics of photovoltaic systems with shaded solar cells,” *Sol. Energy*, vol. 56, no. 6, pp. 513–520, 1996, doi: 10.1016/0038-092X(96)00006-0.
- [25] Janne Viitanen, “Energy efficient lighting systems in buildings with integrated photovoltaics,” *J. Renew. Sustain. Energy*, vol. 6, no. 3, 2015, [Online]. Available: https://scholar.google.com/scholar?as_sdt=2007&q=nen,+J,+Energy+efficient+lighting+systems+in+buildings+with+integrated+photo%3Fvoltaics,+Aaltouniversity,+2015&hl=en
- [26] M. C. Alonso-García, J. M. Ruiz, and F. Chenlo, “Experimental study of mismatch and shading effects in the I-V characteristic of a photovoltaic module,” *Sol. Energy Mater. Sol. Cells*, vol. 90, no. 3, pp. 329–340, 2006, doi: 10.1016/j.solmat.2005.04.022.
- [27] A. C. de W. and W. G. J. H. M. van S. Boudewijn B. Pannebakker, “Photovoltaics in the shade: one bypass diode per Revisited, Cell,” *Wiley Online Libr.*, 2017, doi: 10.1002/pip.2898.
- [28] S. Guo, T. M. Walsh, A. G. Aberle, and M. Peters, “Analysing partial shading of PV modules by circuit modelling,” *Conf. Rec. IEEE Photovolt.*

- Spec. Conf.*, pp. 2957–2960, 2012, doi: 10.1109/PVSC.2012.6318205.
- [29] K. A. Kim and P. T. Krein, “Reexamination of Photovoltaic Hot Spotting to Show Inadequacy of the Bypass Diode,” *IEEE J. Photovoltaics*, vol. 5, no. 5, pp. 1435–1441, 2015, doi: 10.1109/JPHOTOV.2015.2444091.
- [30] V. Sharma and S. S. Chandel, “A novel study for determining early life degradation of multi-crystalline-silicon photovoltaic modules observed in western Himalayan Indian climatic conditions,” *Sol. Energy*, vol. 134, pp. 32–44, 2016, doi: <https://doi.org/10.1016/j.solener.2016.04.023>.
- [31] K. A. Kim and P. T. Krein, “Hot spotting and second breakdown effects on reverse I-V characteristics for mono-crystalline Si Photovoltaics,” in *2013 IEEE Energy Conversion Congress and Exposition, ECCE 2013*, IEEE, 2013, pp. 1007–1014. doi: 10.1109/ECCE.2013.6646813.
- [32] V. Dalessandro, P. Guerriero, and S. Daliento, “A simple bipolar transistor-based bypass approach for photovoltaic modules,” *IEEE J. Photovoltaics*, vol. 4, no. 1, pp. 405–413, 2014, doi: 10.1109/JPHOTOV.2013.2282736.
- [33] K. A. Kim, P. T. Krein, G. S. Seo, and B. H. Cho, “Photovoltaic AC parameter characterization for dynamic partial shading and hot spot detection,” in *Conference Proceedings - IEEE Applied Power Electronics Conference and Exposition - APEC, 2013*, pp. 109–115. doi: 10.1109/APEC.2013.6520194.
- [34] S. Ghazi, A. Sayigh, and K. Ip, “Dust effect on flat surfaces - A review paper,” *Renew. Sustain. Energy Rev.*, vol. 33, pp. 742–751, 2014, doi: 10.1016/j.rser.2014.02.016.
- [35] E. Boykiw, ““The effect of settling dust in the Arava valley on the performance of solar photovoltaic panels.”” Pennsylvania, 2011. [Online]. Available: [https://scholar.google.com/scholar?lookup=0&q=+Boykiw+E.+The+effect+of+settling+dust+in+the+Arava+valley+on+the+performance+of+solar+photovoltaic+panels.+Department+of+Environmental+Science+Allegheny+College+Meadville,+Pennsylvania+\(April+2011\)%3B+2011&hl](https://scholar.google.com/scholar?lookup=0&q=+Boykiw+E.+The+effect+of+settling+dust+in+the+Arava+valley+on+the+performance+of+solar+photovoltaic+panels.+Department+of+Environmental+Science+Allegheny+College+Meadville,+Pennsylvania+(April+2011)%3B+2011&hl)
- [36] M. K. Mazumder, R. Sharma, A. S. Biris, J. Zhang, C. Calle, and M. Zahn, “Self-cleaning transparent dust shields for protecting solar panels and other

- devices,” *Part. Sci. Technol.*, vol. 25, no. 1, pp. 5–20, 2007, doi: 10.1080/02726350601146341.
- [37] E. Klugmann-Radziemska, “Degradation of electrical performance of a crystalline photovoltaic module due to dust deposition in northern Poland,” *Renew. Energy*, vol. 78, pp. 418–426, 2015, doi: 10.1016/j.renene.2015.01.018.
- [38] A. O. Mohamed and A. Hasan, “Effect of Dust Accumulation on Performance of Photovoltaic Solar Modules in Sahara Environment,” *J. Basic. Appl. Sci. Res.*, vol. 2, no. 11, pp. 11030–11036, 2012.
- [39] A. G. Yassine Charabi, “Spatio-temporal assessment of dust risk maps for solar energy systems using proxy data, *Renewable Energy*,” 2012. doi: <https://doi.org/10.1016/j.renene.2011.12.005>.
- [40] M. Gostein, T. Duster, and C. Thuman, “Accurately measuring PV soiling losses with soiling station employing module power measurements,” *2015 IEEE 42nd Photovolt. Spec. Conf. PVSC 2015*, 2015, doi: 10.1109/PVSC.2015.7355993.
- [41] D. A. R. Barkhouse, O. Gunawan, T. Gokmen, T. K. Todorov, and D. B. Mitzi, “Yield predictions for photovoltaic power plants: empirical validation, recent advances and remaining uncertainties,” *Prog. Photovoltaics Res. Appl.*, vol. 20, no. 1, pp. 6–11, 2015, doi: 10.1002/pip.
- [42] A. Y. Al-hasan and A. A. Ghoneim, “A new correlation between photovoltaic panel’s efficiency and amount of sand dust accumulated on their surface,” *Int. J. Sustain. Energy*, vol. 24, no. 4, pp. 187–197, 2005, doi: 10.1080/14786450500291834.
- [43] M. R. Maghami, H. Hizam, C. Gomes, M. A. Radzi, M. I. Rezadad, and S. Hajjighorbani, “Power loss due to soiling on solar panel: A review,” *Renew. Sustain. Energy Rev.*, vol. 59, pp. 1307–1316, 2016, doi: 10.1016/j.rser.2016.01.044.
- [44] H. Jiang, L. Lu, and K. Sun, “Experimental investigation of the impact of airborne dust deposition on the performance of solar photovoltaic (PV) modules,” *Atmos. Environ.*, vol. 45, no. 25, pp. 4299–4304, 2011, doi: 10.1016/j.atmosenv.2011.04.084.

- [45] A. Sayyah, M. N. Horenstein, and M. K. Mazumder, “Energy yield loss caused by dust deposition on photovoltaic panels,” *Sol. Energy*, vol. 107, pp. 576–604, 2014, doi: 10.1016/j.solener.2014.05.030.
- [46] H. Hanifi, M. Pander, B. Jaeckel, J. Schneider, A. Bakhtiari, and W. Maier, “A novel electrical approach to protect PV modules under various partial shading situations,” *Sol. Energy*, vol. 193, no. July, pp. 814–819, 2019, doi: 10.1016/j.solener.2019.10.035.
- [47] “r.sun.” <https://grass.osgeo.org/grass82/manuals/r.sun.html>
- [48] “Solar analyst.” <https://solargis.com/products/analyst/overview>
- [49] “pvsol.” <https://valentin-software.com/en/products/pvsol-premium/>
- [50] I. Reda and A. A. Nrel, “Solar Position Algorithm for Solar Radiation Applications (Revised),” *Natl. Renew. Energy Lab. Nrel/Tp-560-34302*, no. January, pp. 1–56, 2005.
- [51] H. Vogt, M. Hendrix, P. Nenzi, and D. Warning, “Ngspice User ’ s Manual Version 36 (ngspice release version) How to use this Manual,” vol. 36, 2022.